Cystinosin, the small GTPase Rab11, and the Rab7 effector RILP regulate intracellular trafficking of the chaperone-mediated autophagy receptor LAMP2A

Received for publication, October 20, 2016, and in revised form, April 28, 2017 Published, Papers in Press, May 2, 2017, DOI 10.1074/jbc.M116.764076

Jinzhong Zhang[‡], Jennifer L. Johnson[‡], Jing He[‡], Gennaro Napolitano[‡], Mahalakshmi Ramadass[‡1], Celine Rocca[§], William B. Kiosses[‡], Cecilia Bucci[¶], Qisheng Xin[‖], Evripidis Gavathiotis[‖], Ana María Cuervo**, Stephanie Cherqui[§], and Sergio D. Catz[‡2]**

*From the [‡]Department of Molecular Medicine, The Scripps Research Institute, La Jolla, California 92037, the [§]Department of Pediatrics, Division of Genetics, University of California, San Diego, La Jolla, California 92093-0734, the [¶]Department of Biological and Environmental Sciences and Technologies (DiSTeBA), University of Salento, Via Provinciale Monteroni n. 165, 73100 Lecce, Italy, and the Departments of [‖]Biochemistry and **Developmental and Molecular Biology, Albert Einstein College of Medicine, Bronx, New York 10461*

Edited by Thomas Söllner

The lysosomal storage disease cystinosis, caused by cystinosin deficiency, is characterized by cell malfunction, tissue failure, and progressive renal injury despite cystine-depletion therapies. Cystinosis is associated with defects in chaperone-mediated autophagy (CMA), but the molecular mechanisms are incompletely understood. Here, we show CMA substrate accumulation in cystinotic kidney proximal tubule cells. We also found mislocalization of the CMA lysosomal receptor LAMP2A and impaired substrate translocation into the lysosome caused by defective CMA in cystinosis. The impaired LAMP2A trafficking and localization were rescued either by the expression of wild-type cystinosin or by the disease-associated point mutant CTNS-K280R, which has no cystine transporter activity. Defective LAMP2A trafficking in cystinosis was found to associate with decreased expression of the small GTPase Rab11 and the Rab7 effector RILP. Defective Rab11 trafficking in cystinosis was rescued by treatment with small-molecule CMA activators. RILP expression was restored by up-regulation of the transcription factor EB (TFEB), which was down-regulated in cystinosis. Although LAMP2A expression is independent of TFEB, TFEB up-regulation corrected lysosome distribution and lysosomal LAMP2A localization in *Ctns*$^{-/-}$ cells but not Rab11 defects. The up-regulation of Rab11, Rab7, or RILP, but not its truncated form RILP-C33, rescued LAMP2A-defective trafficking in cystinosis, whereas dominant-negative Rab11 or Rab7 impaired LAMP2A trafficking. Treatment of cystinotic cells with a CMA activator increased LAMP2A localization at the lysosome and increased cell survival. Altogether, we show that LAMP2A trafficking is regulated by cystinosin, Rab11, and RILP and that CMA up-regulation is a potential clinically relevant mechanism to increase cell survival in cystinosis.

Lysosomal storage disorders (LSDs),[3] a group of ~50 rare inherited metabolic diseases caused by defects in lysosomal function, are characterized by lysosomal overload and by several associated cellular defects, including increased endoplasmic reticulum (ER) stress, defective autophagy, and cell death. Although individually the incidence of LSD occurrence is ~1:100,000, the incidence, as a group, is about 1:5,000. Cystinosis is a LSD caused by genetic defects in the *CTNS* gene, which codes for cystinosin, the lysosomal cystine transporter (1). These defects cause the anomalous accumulation of the amino acid cystine in lysosomes leading to cell malfunction affecting kidneys, eyes, muscle, liver, and brain (2). As with most LSDs, this leads to a slow but irreversible deterioration, organ dysfunction, and death. The treatment of choice for cystinosis is cysteamine, which reduces the intra-lysosomal level of cystine, retards the rate of glomerular deterioration, and improves linear growth in children with cystinosis. However, even treated patients eventually need transplantation and have a short life expectancy. Thus, despite the efficiency of cysteamine in decreasing lysosomal overload, cell malfunction, progressive renal injury, and tissue failure occur despite cystine depletion therapy (3), suggesting that cystine accumulation is not the only cause for all the defects in cystinosis (3, 4).

CTNS encodes a 367-amino acid protein with seven-transmembrane domains. Several mutations in the *CTNS* gene have been associated with the development of three different onsets

This work was supported by National Institutes of Health USPHS Grants HL088256 and GM105894 (to S. D. C.), by Cystinosis Research Foundation fellowships (to J. Z. and J. H.), by National Institutes of Health Grant R01-DK090058 (to S. C.), by a Michael J. Fox Foundation (MJFF) grant (to A. M. C. and E. G.), and by the generous support of R&R Belfer (to A. M. C.). The authors declare that they have no conflicts of interest with the contents of this article. The content is solely the responsibility of the authors and does not necessarily represent the official views of the National Institutes of Health.

This article contains supplemental Movies S1–S6 and Fig. S1.

[1] Fellow of the American Heart Association.

[2] To whom correspondence should be addressed: Dept. of Molecular Medicine, The Scripps Research Institute, 10550 North Torrey Pines Rd., La Jolla, CA 92037. Tel.: 858-784-7932, Fax: 858-784-2054; E-mail: scatz@scripps.edu.

[3] The abbreviations used are: LSD, lysosomal storage disorder; TFEB, transcription factor EB; MTT, 3-(4,5-dimethylthiazol-2-yl)-2,5-diphenyltetrazolium bromide; ER, endoplasmic reticulum; CMA, chaperone-mediated autophagy; qPCR, quantitative PCR; MEF, mouse embryo fibroblast; DN, dominant-negative; TIRF, total internal reflection fluorescence; TIRFM, TIRF microscopy; EGFP, enhanced GFP.

of cystinosis. The most severe form, infantile cystinosis, is manifested early in life and is characterized by the development of renal Fanconi syndrome and early kidney and corneal complications. In addition, cystine accumulation in patients with infantile cystinosis eventually leads to retinal, endocrinological, hepatic, gastrointestinal, muscular, and neurological anomalies (5). The juvenile form of the disease is manifested by an onset of photophobia and defective glomerular function during adolescence. Finally, ocular non-nephropathic cystinosis is characterized by mild photophobia without renal anomalies. An extensive and comprehensive genetic correlation between mutations in the *CTNS* gene, the cystine transporter activity of cystinosin, and the clinical manifestations of the disease have been previously described by Antignac and co-workers (5). Interestingly, although most genetic defects leading to loss-of-function cause the more severe form of the disease, infantile cystinosis, some mutants with abolished cystine transport activity are associated with the milder phenotype of juvenile cystinosis (5). These data suggest that CTNS may carry out currently unknown functions that are relevant for disease development.

Autophagic pathways are essential cellular processes that consist of the digestion of cellular components through lysosomal degradation (6). Under resting conditions, autophagy represents a quality control mechanism that ensures degradation of long-lived proteins and damaged organelles. However, in response to different stresses, including starvation, the activation of these pathways also promotes cell survival by providing cells with amino acids and nutrients (7). CMA is a selective form of autophagy through which specific cytoplasmic proteins containing a recognition motif (biochemically related to the pentapeptide KFERQ) are bound by a cytoplasmic chaperone complex and delivered to a lysosomal receptor, which mediates the translocation of these CMA substrates into the lysosomal lumen for degradation (8). To date, the only known lysosomal receptor for CMA is LAMP2A, one of the three spliced variants encoded by the *lamp2* gene and the only isoform required for CMA function (9, 10). LAMP2A is dispensable for other types of autophagy (9–11). Substrate binding to LAMP2A is limiting for CMA, and cells use changes in LAMP2A levels to up-regulate or down-regulate CMA (9, 10, 12). Changes in the rate of LAMP2A synthesis, its regulation by degradation, and its subcompartmentalization and organization at the lysosome all contribute to modulation of CMA activity (8). However, the exact mechanisms regulating LAMP2A trafficking, dynamics changes at the lysosomal membrane, and lysosomal localization are not completely elucidated.

CMA accounts for the digestion of a significant amount of the proteome (8) and is particularly important in protein elimination under oxidative stress, a condition markedly elevated in cystinosis (4, 13, 14). Defective CMA is directly linked to human disease, including kidney pathologies (15–17), an organ in which CMA is markedly active (15, 18). In previous studies, we revealed a defective mechanism of CMA in cystinosis (19). We showed abnormal expression levels and localization of the CMA receptor LAMP2A in cystinotic cells and defective lysosomal degradation of CMA substrates in cystinotic lysosomes. Defective CMA was rescued by expression of wild-type cystinosin but not by treatment with cysteamine, although both approaches significantly decreased lysosomal overload (19). Thus our data showed that CMA impairment is an important contributor to the pathogenesis of cystinosis by a mechanism that is independent of lysosomal overload (19), highlighting a possible role of CTNS independent of its cystine transporter activity and underlining the need for complementary treatments to substrate-depletion therapies in cystinosis. In this work, we characterize a novel mechanism of CMA regulation by CTNS, which facilitates LAMP2A trafficking, lysosomal localization, and function. Furthermore, we present evidence that treatment with small-molecule CMA activators increases survival of cystinotic cells independently of lysosomal overload, thus highlighting possible novel treatments for cystinosis through improvement of CMA.

Results

Cystinotic cells are characterized by mislocalization of the CMA receptor, LAMP2A, with normal LAMP1 distribution at lysosomes and impaired CMA activity (19), but *in vivo* defective mislocalization of LAMP2A has not been demonstrated, and the discrete steps during CMA-mediated substrate processing that are impaired in cystinosis have not been elucidated. Here, we first analyzed LAMP2A distribution in disease-relevant kidney proximal tubule cells, the main target of cystinosis. In Fig. 1*A*, we show that proximal tubule cells from $Ctns^{-/-}$ mice show apical distribution of LAMP2A but the absence of the lysosomal protein in basal areas of the proximal tubule cells. To determine whether LAMP2A mislocalization is associated with the deficient processing of CMA substrates, we next analyzed endogenous levels of the CMA substrate GAPDH by quantitative immunofluorescence analysis. In Fig. 1*B*, we show CMA substrate accumulation in tissues from $Ctns^{-/-}$ mice indicating, for the first time, abnormal CMA in CTNS-deficient proximal tubule cells. Next, we use a quantitative super-resolution microscopy approach to study the defective LAMP2A localization at the lysosomal membrane. We show that LAMP2A localizes at micro-domains that are characterized by the adjacent distribution of LAMP1 in wild-type cells (Fig. 1*C*). Next, we demonstrate that in cystinotic cells, LAMP2A localizes at micro-domains that are different from those enriched in the lysosomal membrane-associated protein LAMP1 (Fig. 1*C*). To unequivocally determine the localization of LAMP2A relative to LAMP1, quantitative analysis after drift correction indicates that although >50% of LAMP2A molecules are located at distances that are <100 nm from LAMP1-positive micro-domains in wild-type cells, cystinotic cells show a significantly decreased number (<20%) of LAMP2A molecules present at these lysosomal membrane micro-domains (Fig. 1*D*).

Because the correct distribution of LAMP2A at the lysosomal membrane and its proper molecular multimerization and association with lysosomal membrane proteins regulate its susceptibility to degradation and function (20), we next hypothesized that the defective lysosomal distribution of LAMP2A in cystinotic cells may lead to impaired substrate internalization into the lysosome. To determine whether CMA defects in cystinosis is caused by impaired translocation of the CMA substrate into the lysosomal lumen due to decreased LAMP2A, we analyzed CMA activity (Fig. 1*E*, *red box*) and CMA substrate

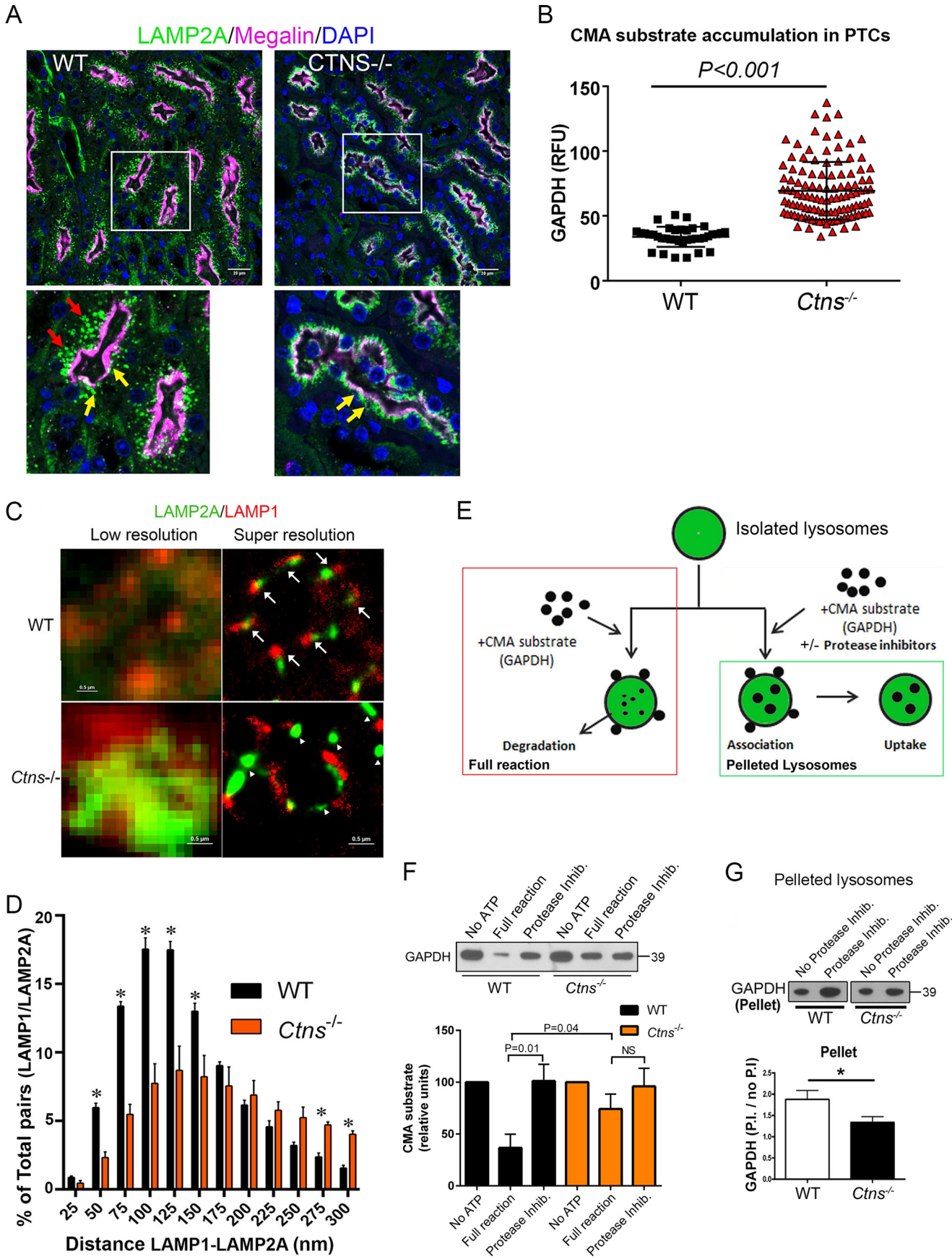
A
LAMP2A/Megalin/DAPI
WT
CTNS-/-
B
CMA substrate accumulation in PTCs
P<0.001
GAPDH (RFU)
150
100
50
0
WT
Ctns-/-
C
LAMP2A/LAMP1
Low resolution
Super resolution
WT
Ctns-/-
0.5 µm
D
% of Total pairs (LAMP1/LAMP2A)
20
15
10
5
0
25
50
75
100
125
150
175
200
225
250
275
300
Distance LAMP1-LAMP2A (nm)
WT
Ctns-/-
E
Isolated lysosomes
+CMA substrate
(GAPDH)
+CMA substrate
(GAPDH)
+/- Protease inhibitors
Degradation
Full reaction
Association
Uptake
Pelleted Lysosomes
F
No ATP
Full reaction
Protease Inhib.
GAPDH
39
WT
Ctns-/-
CMA substrate
(relative units)
P=0.04
P=0.01
NS
G
Pelleted lysosomes
No Protease Inhib.
Protease Inhib.
GAPDH
(Pellet)
Pellet
GAPDH (P.I. / no P.I)

translocation into the lysosomal lumen (Fig. 1*E*, *green box*) using an assay that is considered the gold standard for testing CMA (21). We optimized this assay to obtain CMA-active lysosomes, whose integrity was verified by measuring β-hexosaminidase activity in purified lysosomes compared with burst lysosomes, as described previously (19). In the presence of functional intraluminal proteases, internalized substrate is readily degraded, and therefore external, membrane-bound, and undigested internalized GAPDH can be detected in the full reactions (Fig. 1*E*, *red box*). For translocation assays, lysosomes are incubated with GAPDH in the presence or absence of protease inhibitors and spun down before analysis. Lysosomal membrane-bound and translocated substrate is accumulated in the presence of protease inhibitors (Fig. 1*E*, *green box*). Thus, the ratio between the amount of pelleted GAPDH in the presence of protease inhibitors *versus* the amount in the absence of proteases reflects the rate of substrate translocation into the lysosomal lumen. Importantly, the expression levels of LAMP2A are decreased in *Ctns*$^{-/-}$ lysosomes purified from mouse liver (19). First, we confirmed defective CMA in cystinotic lysosomes using the full reaction (Fig. 1*F*). Next, to define whether impaired CMA could be caused by defective binding or translocation of the CMA substrates, intact lysosomes were incubated with the CMA substrate GAPDH and pelleted, and the levels of lysosome-associated GAPDH were evaluated in the presence or absence of protease inhibitors. As shown in Fig. 1*G*, the levels of GAPDH associated with WT lysosomes were increased in the presence of protease inhibitors compared with full reactions, indicating active substrate internalization. In contrast, although in full reactions the levels of GAPDH bound to *Ctns*$^{-/-}$ lysosomes were similar to those bound to WT lysosomes, the amount of GAPDH associated with *Ctns*$^{-/-}$ lysosomes increased only slightly in the presence of protease inhibitors (Fig. 1*G*), indicating that cystinotic lysosomes are characterized by functional binding but impaired translocation of CMA substrates. Of note, impaired substrate degradation by lysosomes from *Ctns*$^{-/-}$ cells is not caused by defective lysosomal proteases (19). Altogether, our data show for the first time that impaired localization of LAMP2A at the lysosomal membrane in cystinotic cells is associated with defective substrate translocation into the lysosomal lumen.

CTNS expression but not treatment with cysteamine rescued the localization of LAMP2A at the lysosomal membrane (19), suggesting that CTNS may directly regulate LAMP2A trafficking. Here, to study whether LAMP2A localization depends on the cystine transporter activity of CTNS, we used the mutant CTNS^{K280R} with abolished cystine transporter activity (Fig. 2*A*). This mutation is manifested in patients with cystinosis and produces a protein that, although unable to reduce lysosomal overload, retains lysosomal localization (5). Both wild-type CTNS and its mutant CTNS^{K280R} localize at LAMP1-positive structures in both wild-type and cystinotic cells (Fig. 2, *B–D*). We analyzed the localization of endogenous LAMP2A in wild-type, cystinotic, and cystinotic cells expressing exogenous wild-type CTNS or the CTNS^{K280R} mutant and show that the expression of either wild-type protein or CTNS^{K280R} equally rescues the LAMP2A localization-defective phenotype in cystinosis (Fig. 2, *C* and *D*), suggesting that cystinosin itself is a cofactor necessary for LAMP2A sorting or trafficking. Further confirmation of these results comes from quantitative analysis showing that although the colocalization of LAMP1 and LAMP2A is impaired in cystinotic cells, this defect is corrected when the expression of either wild-type CTNS or the CTNS^{K280R} mutant is reconstituted in cystinotic cells (Fig. 2*E*). Thus, the observation that CTNS and CTNS^{K280R} are similarly effective in rescuing the defective phenotype further supports the idea that CTNS mediates important lysosomal functions in addition to, and independently of, its role as the only cystine transporter in the lysosome.

Next, to better understand the molecular mechanism of CTNS-mediated LAMP2A localization at the lysosomal membrane, we analyzed the effect of the CTNS isomeric form CTNS-LKG on LAMP2A subcellular distribution. In CTNS-LKG, the canonical tyrosine-based motif (GYDQL) located in the C-terminal tail is replaced by a 38-amino acid stretch (22, 23). In Fig. 2, *E* and *F*, we show that similar to CTNS and CTNS^{K280R}, CTNS-LKG rescues the LAMP2A mislocalization

Figure 1. LAMP2A mislocalization is associated with *in vivo* accumulation and impaired CMA substrate lysosomal internalization in cystinosis. *A* and *B, in vivo* mislocalized LAMP2A and increased CMA substrate accumulation in *Ctns*$^{-/-}$ mouse PTCs. *A,* immunofluorescence analysis of mouse PTCs, identified by the expression of the apical receptor megalin (*pink*), shows that in contrast to WT PTCs (*left panels*), *Ctns*$^{-/-}$ PTCs (*right panels*) have apical (*yellow arrows*) but not basal (*red arrows*) localization of LAMP2A. Representative images from 45 and 37 fields analyzed from two wild-type and three *Ctns*$^{-/-}$ mice, respectively. *B,* LAMP2A mislocalization is associated with increased accumulation of the CMA substrate GAPDH in *Ctns*$^{-/-}$ PTCs. Quantification of fluorescence intensity from 39 and 47 fields analyzed from two wild-type and three *Ctns*$^{-/-}$ mice. All fields were randomly selected by "tiling and stitching." *C,* super-resolution microscopy analysis of LAMP1 (*red*) and LAMP2A (*green*) distribution in wild-type and *Ctns*$^{-/-}$ lysosomes. The *arrows* show LAMP2A localization adjacent to LAMP1 molecules in wild-type cells. *Arrowheads* show LAMP2A molecules at micro-domains distant from LAMP1 molecules. *D,* quantitative analysis of the distribution of LAMP2A relative to LAMP1 molecules as determined by STORM. Quantification of the distance between LAMP1 and LAMP2A centroids was performed as described under "Materials and methods." A total of 30,486 and 13,985 LAMP1-LAMP2A pairs were analyzed for WT and *Ctns*$^{-/-}$ cells, respectively. Results are expressed by binning the distance between pairs in 25-nm increments and plotted as a percentage of total pairs at the given distance for each cell. A total of three cells for each condition were analyzed. dSTORM images were processed using Nikon software to correct for drift during acquisition as described under "Materials and methods." Mean ± S.E. *, $p < 0.05$. *E,* schematic representation of lysosomal isolation and *in vitro* CMA assay. The scheme represents the analysis of CMA activity (*red box*) and CMA substrate translocation into the lysosomal lumen (*green box*). *F,* lysosomes were isolated from livers of starved wild-type (*WT*) and *Ctns*$^{-/-}$ mice, and CMA activity was measured by incubation for 30 min with the CMA substrate GAPDH. GAPDH degradation was analyzed by Western blotting. CMA activity was measured by analysis of the remaining levels of GAPDH in the full reaction (maximal degradation, *red box* in *E*). Controls consisting of reactions performed in the absence of ATP (which is necessary for CMA activity) or in the presence of protease inhibitors (*Protease Inhib.*) were run in parallel. Quantitative densitometry results are shown. Mean ± S.E. ($n = 7$). *NS,* not significant (unpaired *t* test). *G,* CMA reactions were carried out in the presence or absence of protein inhibitors; then lysosomes were pelleted (*green box* in *E*); and the amount of GAPDH bound to the lysosomal membrane and/or internalized into the lysosomal lumen were assessed by Western blotting. Quantitative densitometry analysis shows the ratio between the amounts of GAPDH in the presence of protease inhibitors (*P.I.*) (bound and internalized GAPDH) *versus* in the absence of protease inhibitors (*no P.I.*) (bound GAPDH). Results are mean ± S.E. ($n = 4$). *, $p < 0.05$ (unpaired *t* test).

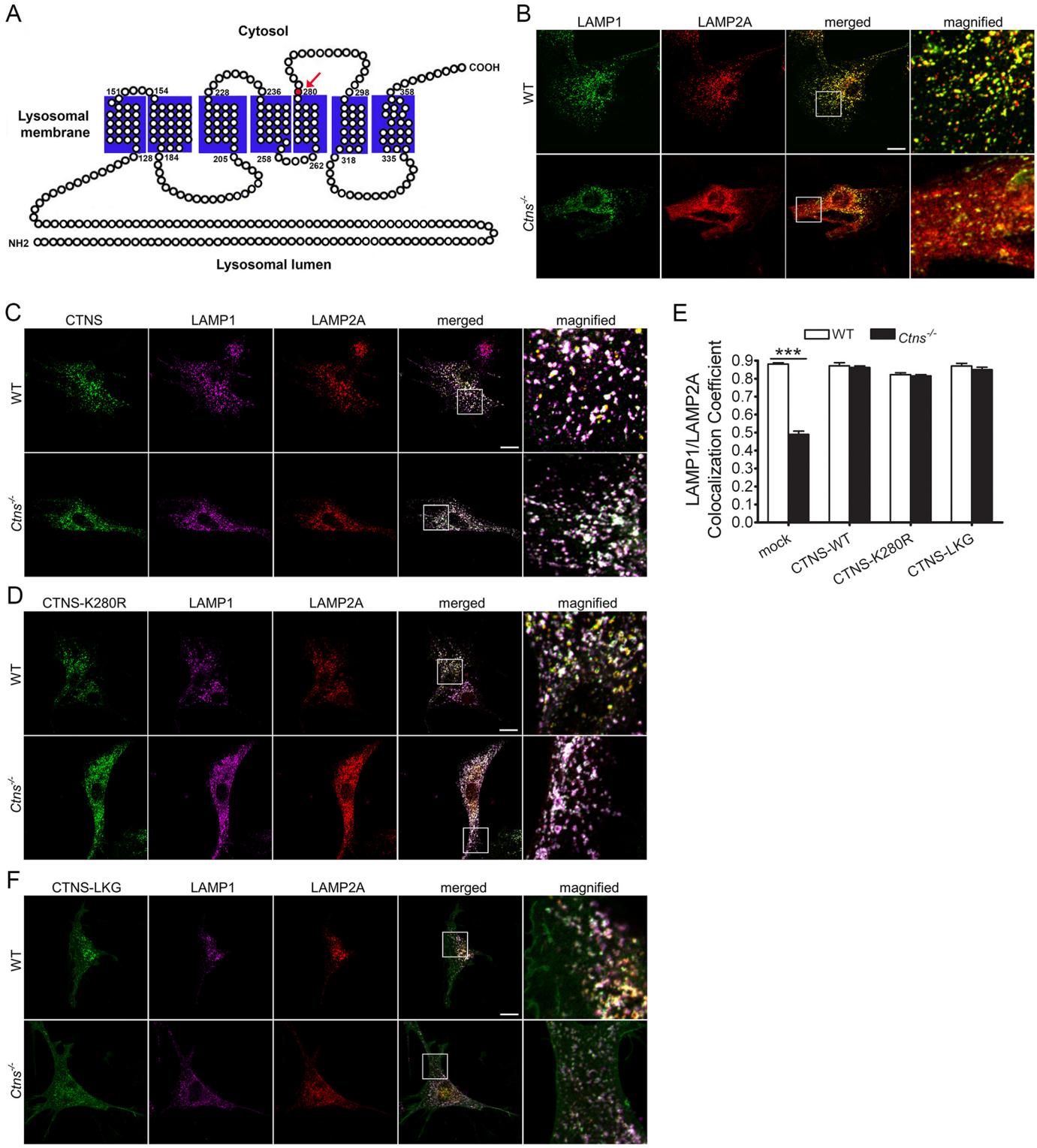

Figure 2. Cystine transporter-inactive CTNS mutant CTNS^{K280R} rescues the localization of the CMA receptor, LAMP2A, at the lysosomal membrane of cystinotic cells. *A,* schematic representation of the human CTNS protein. The mutant residue Lys-280, which is mutated to an arginine in the disease-associated mutant CTNS^{K280R}, is indicated with an *arrow*. The K280R abolishes the cystine transporter activity of CTNS. This mutation is manifested in patients with cystinosis and produces a protein that, although incapable of reducing lysosomal overload, retains lysosomal localization. *B–D,* immunofluorescence analysis of the localization of LAMP1 and LAMP2A in cells expressing either GFP-CTNS or GFP-CTNS^{K280R} mutant in wild-type (*WT*) or *Ctns*$^{-/-}$ cells. Triple colocalization between LAMP1, LAMP2A, and CTNS (*white*) can be observed in merged and magnified images. *Scale bars,* 20 μm. *E,* quantitative analysis of the colocalization of LAMP2A and LAMP1 in wild-type cells (WT, *white columns*) or *Ctns*$^{-/-}$ cells (*black columns*) expressing either GFP-CTNS (CTNS-WT), GFP-CTNS^{K280R}, or GFP-CTNS-LKG. *F,* immunofluorescence analysis of the localization of LAMP1 and LAMP2A in cells expressing GFP-CTNS-LKG variant in wild-type (*WT*) or *Ctns*$^{-/-}$ cells. *B–F,* triple colocalization between LAMP1, LAMP2A, and CTNS (*white*) can be observed in merged and magnified images. *Scale bars,* 20 μm. The data represent the mean ± S.E. of three independent experiments.

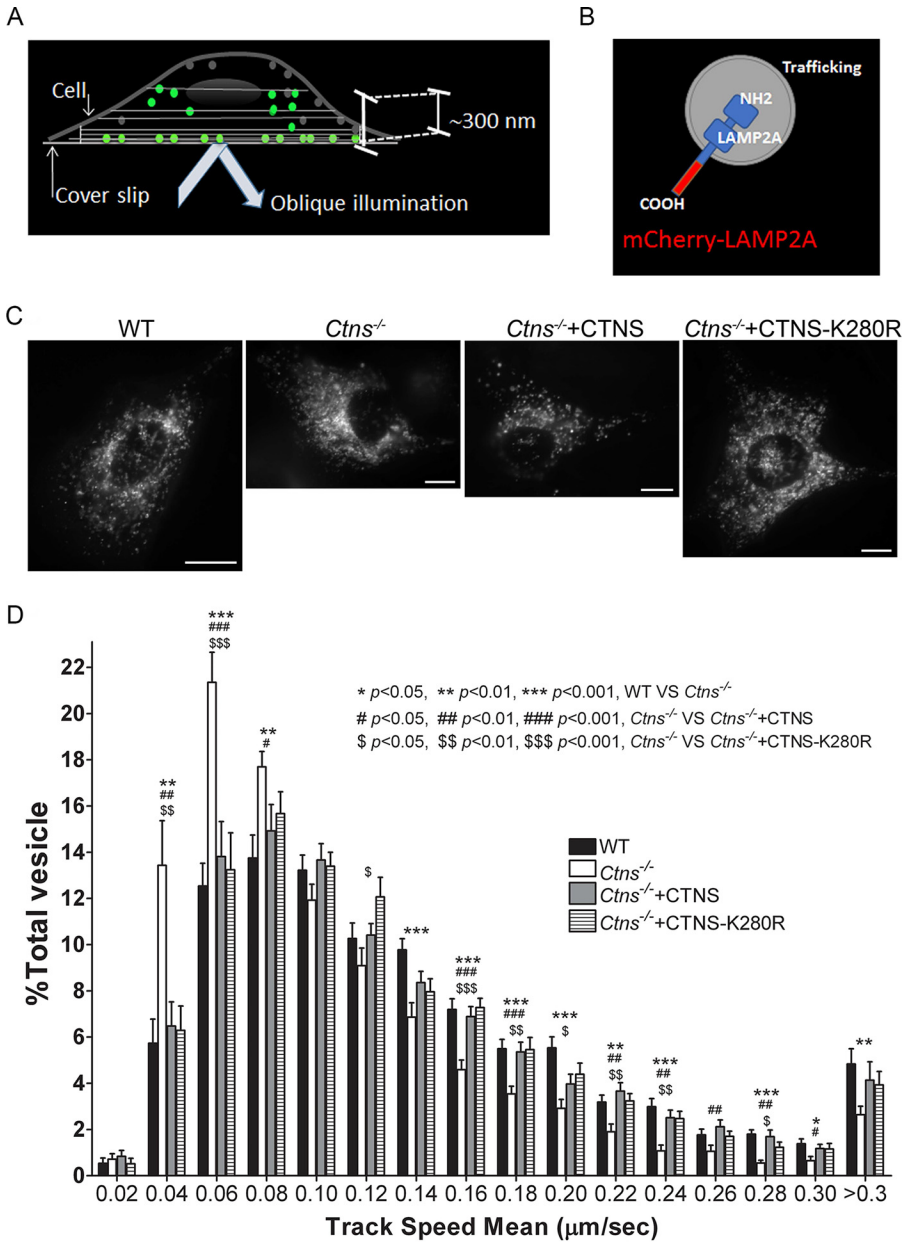

Figure 3. CTNS regulates LAMP2A trafficking. *A,* schematic representation of pseudo-TIRFM, a technique widely used to study vesicular trafficking (24, 25). Different from conventional TIRFM, pseudo-TIRFM facilitates the analysis of organelles that may not necessarily be in areas adjacent to the plasma membrane (beyond 100 nm), while maintaining an excellent signal to background ratio (26). *B,* schematic representation of the LAMP2A protein used in trafficking studies. The C terminus of LAMP2A was tagged with mCherry. The mCherry tag in this position does not affect LAMP2A localization (27). *C,* representative images of cells used in trafficking studies. *Scale bar,* 10 μm. *D,* quantitative analysis of the trafficking of LAMP2A in wild-type (*WT*), *Ctns*$^{-/-}$, or *Ctns*$^{-/-}$ cells reconstituted with either wild-type GFP-CTNS or with its mutant GFP-CTNS^{K280R}. *Histograms* represent the speeds of mCherry-LAMP2A-containing organelles in wild-type cells and cystinotic cells expressing either wild-type CTNS or the mutant CTNS^{K280R}. The speeds for the independent vesicles were binned in 0.02-μm/s increments and plotted as a percentage of total vesicles for a given cell. Results are represented as mean ± S.E. from 20 WT cells, 20 *Ctns*$^{-/-}$ cells, or 20 and 20 *Ctns*$^{-/-}$ cells expressing either wild-type CTNS or CTNS^{K280R}, respectively. The statistically significant differences between the groups are indicated in the figure.

phenotype demonstrating, for the first time, a cystine transporter-independent function for this isoform.

To directly analyze whether CTNS regulates LAMP2A trafficking, LAMP2A dynamics were studied using a high-sensitivity microscopy approach, pseudo-TIRFM, widely used in our and other laboratories to study vesicular trafficking (24, 25). Different from conventional TIRFM, pseudo-TIRFM facilitates the analysis of organelles that may not necessarily be in areas adjacent to the plasma membrane, while maintaining an excellent signal to background ratio (Fig. 3*A*) (26). For this assay, we use a construct for the expression of LAMP2A as an mCherry-tagged protein (generous gift from Dr. Santiago Di Pietro) (Fig. 3*B*) that does not interfere with LAMP2A localization (27), but because its C-terminal tag interferes with substrate recognition, it does not rescue CMA. Our quantitative vesicular dynamics analysis demonstrates that LAMP2A trafficking is defective in *Ctns*$^{-/-}$ cells (Fig. 3, *C* and *D*, and supplemental Movies 1 and 2). Thus, we show that in the absence of CTNS, LAMP2A-positive vesicles move at a relatively slow speed (Fig. 3*D*). In addition, we observed a significantly increased number

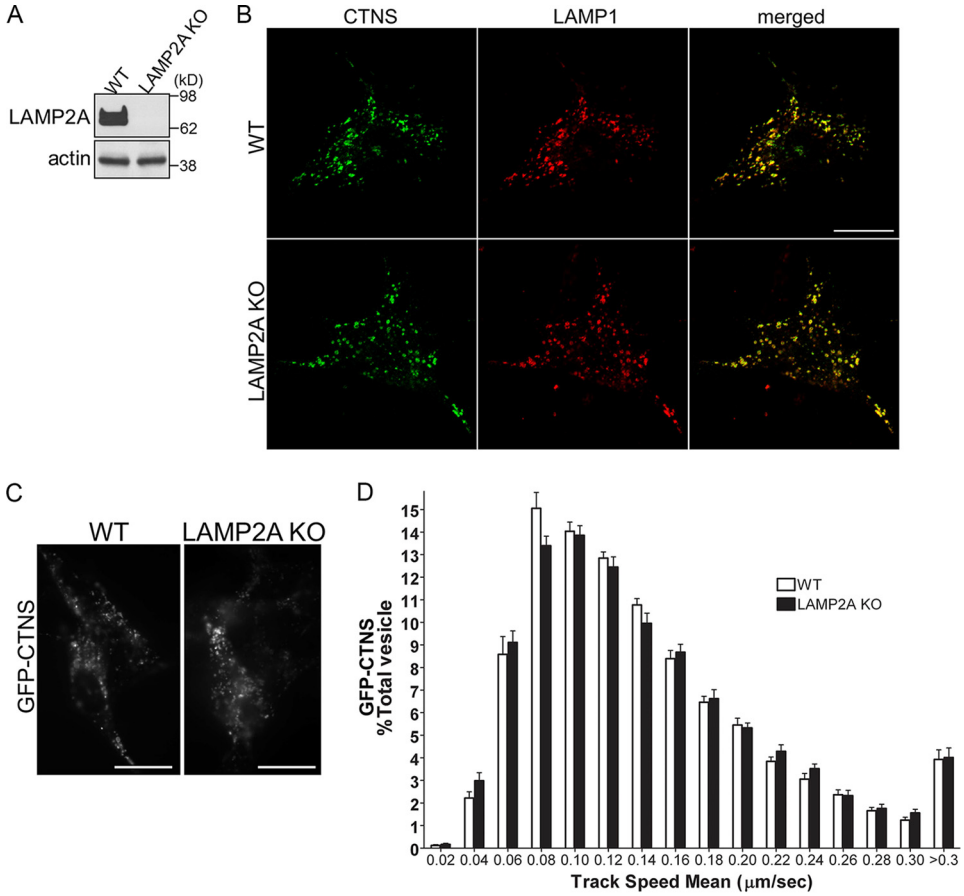

Figure 4. CTNS localization and trafficking is not affected in LAMP2A-deficient cells. *A,* Western blot analysis of LAMP2A in WT and LAMP2A KO MEFs. *B,* representative images of wild-type (*WT*) or LAMP2A-KO MEFs expressing GFP-CTNS. Immunofluorescence analysis of endogenous LAMP1 confirmed that CTNS localization at LAMP1-positive organelles is not affected by LAMP2A down-regulation. *Scale bars,* 20 μm. *C* and *D,* vesicular trafficking of GFP-CTNS-positive organelles was performed by pseudo-TIRFM as described in Fig. 3 legend and under "Materials and methods." *C,* representative images of analyzed cells. *D, histograms* representing the speeds of GFP-CTNS-containing organelles in wild-type cells and LAMP2A-KO cells are shown. The speeds for the independent vesicles were binned in 0.02-μm/s increments and plotted as a percentage of total vesicles for a given cell. Results are represented as mean ± S.E. from 21 WT cells and 21 LAMP2A$^{-/-}$ cells expressing GFP-CTNS. The statistical analysis established no significant differences between groups.

of LAMP2A-positive vesicles with motility restriction (speed under 0.08 μm/s) in *Ctns*$^{-/-}$ cells, thus supporting a possible role for cystinosin in LAMP2A trafficking. Next, to analyze whether the cystine transporter activity of CTNS is important for restoring LAMP2A trafficking, we performed rescued experiments with the CTNS wild-type protein and with the CTNS disease-associated point mutant CTNS^{K280R}. In Fig. 3*D*, we show that both wild-type CTNS and the transporter-deficient mutant CTNS^{K280R} rescue the LAMP2A trafficking-defective phenotype in cystinotic cells (see also supplemental Movies 3 and 4). The defect is not related to cytoskeleton disarray, because super-resolution microscopy analysis shows normal microtubule distribution in *Ctns*$^{-/-}$ cells (supplemental Fig. S1).

To further understand a possible cross-regulation between CTNS and LAMP2A, we next asked whether LAMP2A may be necessary for CTNS trafficking and localization. To this end, we utilized embryonic fibroblasts from LAMP2A-KO mice (MEFs) (Fig. 4*A*) (28, 29) in trafficking and lysosomal protein localization analysis. We analyzed the subcellular localization of CTNS related to that of LAMP1 and show that LAMP2A is not needed for the proper localization of CTNS at lysosomal structures (Fig. 4*B*). In agreement with this observation, the vesicular dynamics of CTNS-positive vesicles is not affected by the absence of LAMP2A expression (Fig. 4, *C* and *D*), suggesting that whereas CTNS is important for LAMP2A trafficking, LAMP2A is dispensable for the correct subcellular localization of CTNS.

Different from the classical distribution of LAMP2A at perinuclear lysosomes, LAMP2A localization in cystinotic cells is characterized by its distribution at small puncta present throughout the cystinotic cells. We have previously shown that LAMP2A localizes at Rab11-positive vesicles in cystinosis cells but not in wild-type cells (19), indicating that the small puncta correspond to Rab11-intermediate carrier vesicles. This is also supported by our previous studies showing that non-lysosomal LAMP2A is not present in VAMP7-positive vesicles and is not retained in the endoplasmic reticulum but colocalizes with Rab11-positive vesicles instead (19).

To analyze the mechanisms that may lead to defective LAMP2A trafficking, we next hypothesized that impaired Rab11-positive vesicle trafficking may be responsible for the defective LAMP2A dynamics. To test this hypothesis, we first analyzed Rab11 expression in wild-type and *Ctns*$^{-/-}$ cells. Quantitative immunoblotting analysis shows that Rab11 expression is down-regulated in cystinotic cells (Fig. 5*A*). Tran-

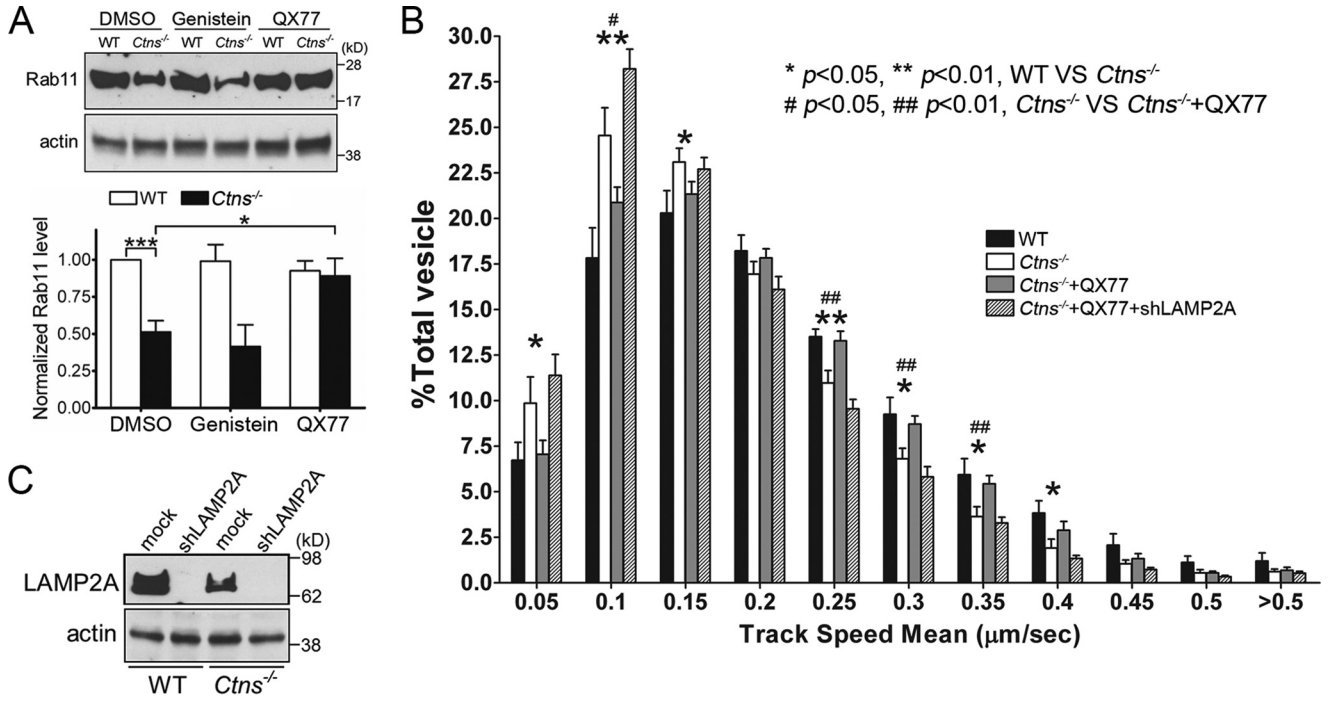

Figure 5. Rab11 is down-regulated in cystinosis and its trafficking is enhanced by CMA activation. *A,* WT and $Ctns^{-/-}$ MEFs were treated with DMSO, genistein, or QX77 for 48 h, and Rab11 expression levels were analyzed by Western blotting. Quantitation of Rab11 expression levels is from three independent experiments. *Error bars* represent S.E. *, $p < 0.05$, and ***, $p < 0.001$, Student's *t* test. *B,* vesicular trafficking of GFP-Rab11-positive organelles was performed by pseudo-TIRFM. *Histograms* represent the speeds of GFP-Rab11-containing organelles in WT and $Ctns^{-/-}$ MEFs. Where indicated, $Ctns^{-/-}$ cells and $Ctns^{-/-}$ cells that were down-regulated for LAMP2A expression were treated with the CMA activator QX77 before analysis. The speeds for the independent vesicles were binned in 0.05-μm/s increments and plotted as a percentage of total vesicles for a given cell. Results are represented as mean ± S.E. from at least 12 cells. The statistically significant differences between the groups are indicated in the figure. *C,* immunoblotting control of LAMP2A expression after down-regulation. WT and $Ctns^{-/-}$ MEFs were infected with lentiviral mouse shRNA against LAMP2A for 7 days. Expression levels of LAMP2A were evaluated by Western blotting.

scriptional regulatory pathways are important to both improve cell function in cystinosis (14) and up-regulate CMA (8). In particular, up-regulation of transcription factor EB (TFEB) rescues some lysosomal abnormalities in cystinosis (30). Furthermore, recently described CMA activators (atypical retinol derivatives) that operate through the release of the endogenous inhibition of the retinoic receptor-α signaling pathway over CMA, up-regulate LAMP2A expression and enhance CMA activity (31). To study whether Rab11 expression could be rescued by TFEB up-regulation or CMA activation, we treated $Ctns^{-/-}$ cells either with genistein, a natural isoflavone present in soy, that activates TFEB (32) or with the CMA activator QX77 (for structure, see United States Patent 9512092 B2) derived from the original AR7 (31). We found that QX77 but not genistein induces the up-regulation of Rab11 expression to the levels observed in wild-type cells (Fig. 5*A*). Of note, QX77 but not genistein also up-regulates LAMP2A expression.

Next, to better understand the defective mechanism induced by the observed Rab11 down-regulation in cystinosis, we analyzed Rab11 trafficking using a GFP-Rab11 chimera transiently expressed in wild-type and cystinotic MEFs. We show that Rab11-positive vesicles are characterized by decreased motility in $Ctns^{-/-}$ cells (Fig. 5*B*) thus linking for the first time CMA defects with impaired vesicular trafficking. Importantly, treatment of cystinotic cells with the CMA activator QX77 shows that Rab11-positive carrier vesicles recover the high-motility trafficking phenotype observe in wild-type cells (Fig. 5*B*).

To determine whether the QX77 effect was dependent on LAMP2A, we next down-regulated LAMP2A expression in wild-type and $Ctns^{-/-}$ cells using largely validated (shRNAs) (Fig. 5*C*). Rab11 vesicular trafficking was rescued by the CMA activator QX77 in cystinotic cells expressing LAMP2A but not in cells down-regulated for the CMA receptor (Fig. 5*B*), suggesting that CMA up-regulation is necessary to stabilize the Rab11-dependent trafficking machinery to then facilitate further Rab11-dependent LAMP2A trafficking.

LAMP2A traffics to the lysosome via several different pathways (33), therefore to dissect the mechanisms responsible for the defective LAMP2A trafficking in cystinosis, we performed mRNA array quantitative analysis using kidneys from wild-type and cystinotic mice. These studies (the full RNA array will be published in a separate work) have identified the down-regulation of the Rab11 effector Rab11-FIP4 (Rab11 Family Interacting Protein 4) in cystinosis, supporting our observations that Rab11-dependent trafficking is defective in this disease. In addition, we found that the expression of the Rab7 effector and late endosome trafficking regulator RILP (Rab-interacting lysosomal protein) was significantly down-regulated in cystinosis (both, $p < 0.01$, $n = 6$) (Fig. 6*A*). Because a significant population of LAMPs traffic to the lysosome via the endocytic pathway (34), we aim to establish whether RILP could regulate LAMP2A trafficking either using the Rab11-dependent or -independent pathways in cystinosis. Quantitative RT-PCR confirmed the down-regulation of *Rilp* RNA in cystinotic fibroblasts (Fig. 6*B*), and Western blot analysis of MEFs confirmed that RILP expression, but not the expression of its binding partner Rab7, is decreased in cystinotic cells (Fig. 6*C*). Importantly, the expression of RILP but not the dominant-negative deletion mutant of

A

ProbeSet	Symbol	Name	Fold Change	Parametric p-value	Gene ID
10378627	Rilp	Rab interacting lysosomal protein	0.61	3.92E-05	280408
10388241	Ctns	Cystinosin	0.51	<1E-07	83429

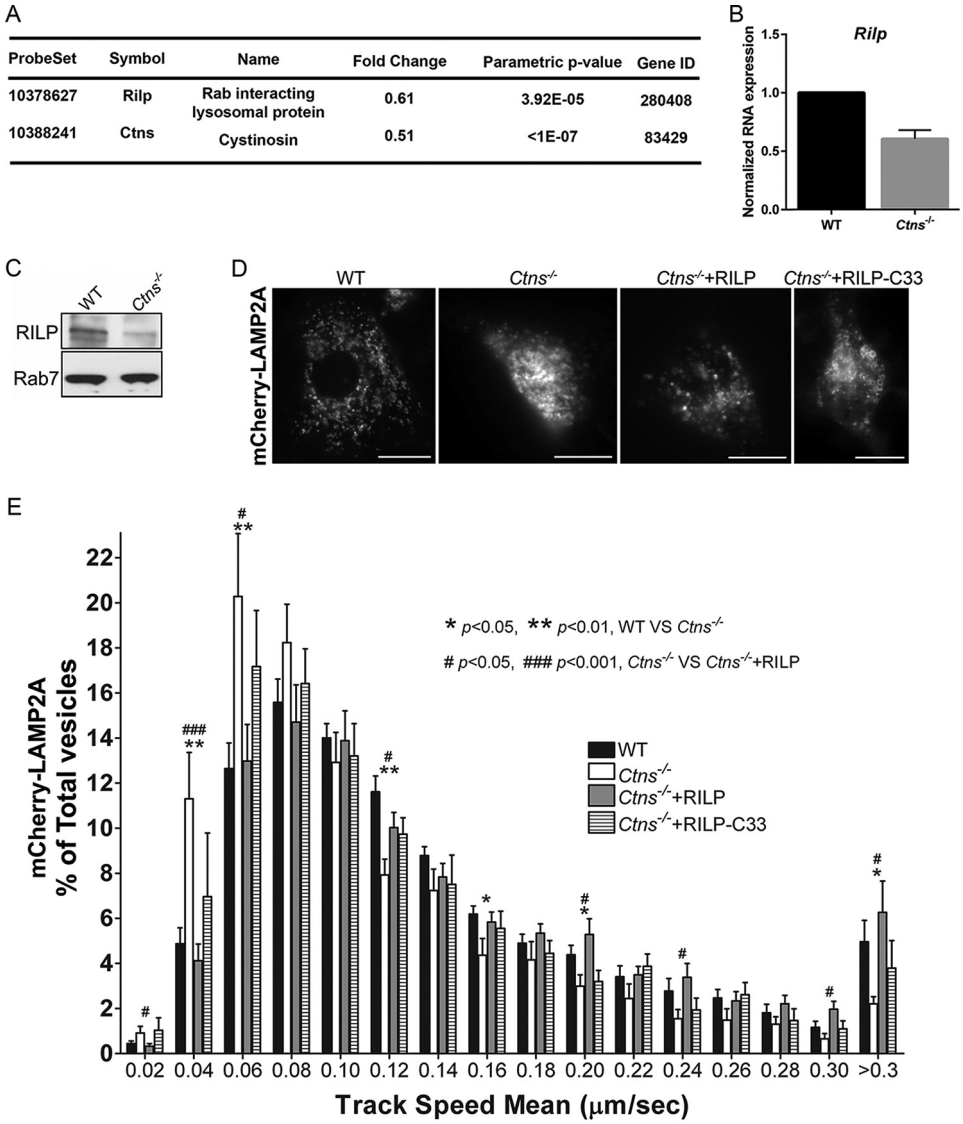

Figure 6. RILP is down-regulated in cystinosis and its expression rescues LAMP2A trafficking. *A,* differential gene expression between wild-type and *Ctns*$^{-/-}$ kidneys from six independent mice was analyzed using a mRNA array as described under "Materials and methods." From the 28,853 genes used for random variance estimation 3,260 were found to be significantly different between classes at the nominal 0.001 level of the univariate test. One of these genes, *Rilp*, a Rab7-binding protein involved in lysosomal trafficking, was significantly down-regulated (fold change indicates gene expression in *Ctns*$^{-/-}$ kidneys *versus* wild-type controls). The values observed for the *Ctns* gene are included as control. *B,* qRT-PCR analysis confirmation of *Rilp* down-regulation in *Ctns*$^{-/-}$ mouse fibroblasts. Mean ± S.D. *C,* Western blot analysis confirmed that RILP, but not its binding partner Rab7, is down-regulated, at the protein level, in cystinotic MEFs. *D* and *E,* RILP expression rescues LAMP2A trafficking in cystinotic cells. Wild-type (*WT*) or *Ctns*$^{-/-}$ MEFs were transfected with mCherry-LAMP2A. Where indicated, the cells were co-transfected for the expression of RILP or RILP-C33 (a truncated form of the protein lacking the N-terminal half). LAMP2A vesicular trafficking was performed by pseudo-TIRFM as described in Fig. 3 legend and under "Materials and methods." *D,* representative images of analyzed cells. *Scale bars,* 20 μm. *E, histograms* representing the speeds of mCherry-LAMP2A-containing organelles in wild-type cells and cystinotic cells expressing either wild-type RILP or RILP-C33 are shown. The speeds for the independent vesicles were binned in 0.02-μm/s increments and plotted as a percentage of total vesicles for a given cell. Results are represented as mean ± S.E. from 20 WT cells, 11 *Ctns*$^{-/-}$ cells, or 17 and 16 *Ctns*$^{-/-}$ cells expressing either wild-type RILP or RILP-C33, respectively. The statistically significant differences between the groups are indicated in the figure.

RILP (RILP-C33) rescued the LAMP2A vesicular dynamics defective phenotype in *Ctns*$^{-/-}$ cells (Fig. 6, *D* and *E,* and supplemental Movies 5 and 6), thus identifying a central role for RILP in LAMP2A trafficking in cystinosis.

Differently from that observed for Rab11, RILP expression was up-regulated by genistein but not by the CMA activator QX77 (Fig. 7*A*), suggesting that the up-regulation of TFEB, a CMA-independent mechanism, may have indirect implications on CMA through the regulation of vesicular trafficking in these cells. To establish a possible expanded mechanism mediated by TFEB on vesicular trafficking regulation, we next studied the distribution of LAMP1-positive organelles in wild-type and *Ctns*$^{-/-}$ cells expressing exogenous TFEB. First, we showed that similar to that observed in PTCs (30), endogenous TFEB is down-regulated in *Ctns*$^{-/-}$ mouse fibroblasts (Fig. 7*B*). Next, we transfected cystinotic cells with either wild-type TFEB or with its constitutively active point mutants TFEB-S3AR4A lacking the N-terminal phosphorylation and 14-3-3-binding site (35), shown previously to mediate transcriptional activity (36). Constitutively active TFEB showed a clear nuclear localization (Fig. 7*C*). The expression of wild-type TFEB or TFEB-S3AR4A increased the perinuclear distribution of both LAMP1

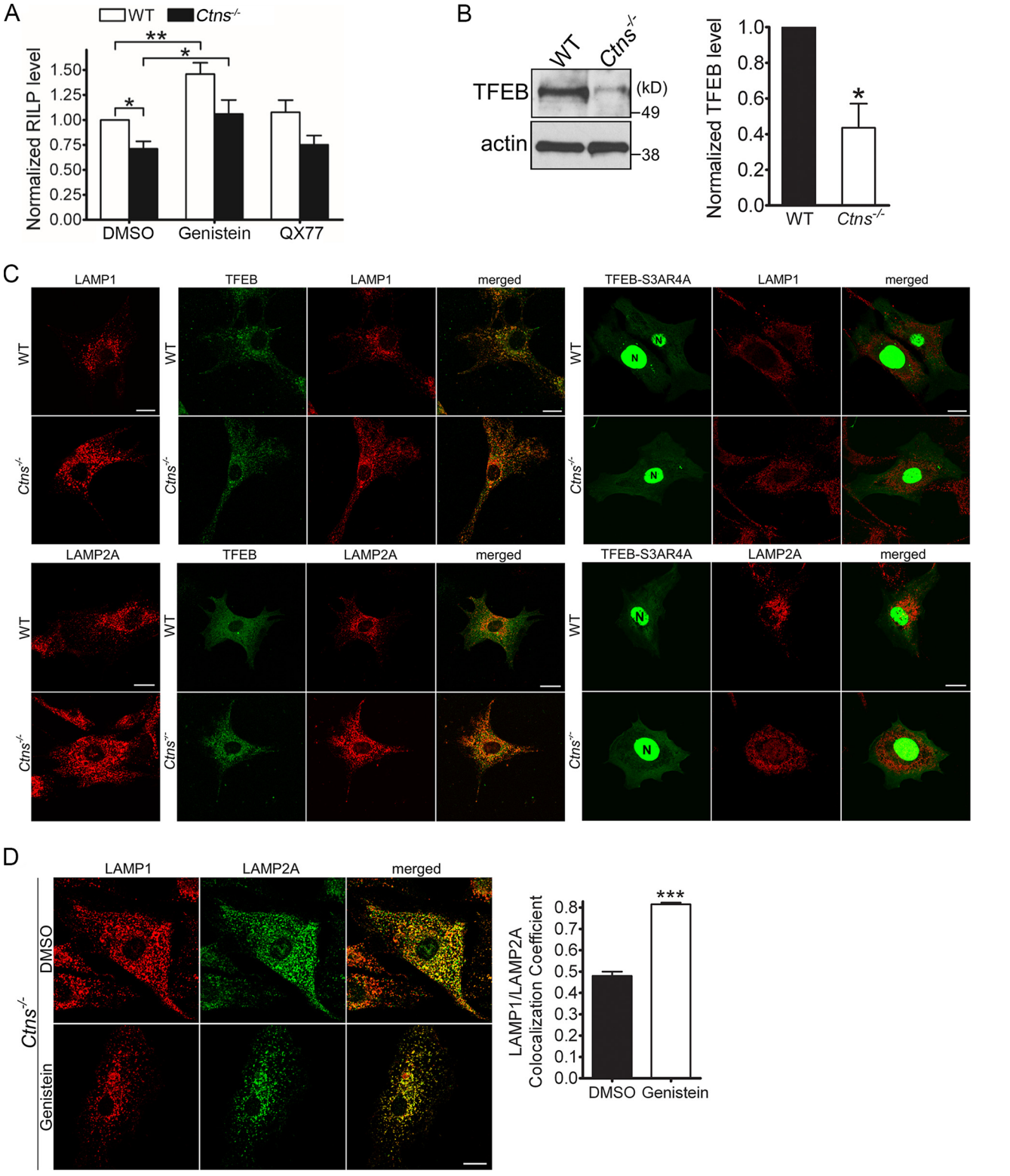

Figure 7. TFEB activation improves lysosomal trafficking and corrects the localization of LAMP2A in cystinotic cells. *A,* WT and CTNS KO MEFs were treated with DMSO, genistein, or QX77 for 48 h, and RILP expression levels were analyzed by qPCR. Quantitation of RILP levels are from three independent experiments. *Error bars* represent S.E. *, $p < 0.05$, and **, $p < 0.01$, Student's *t* test. *B,* TFEB expression is down-regulated in cystinotic cells. Western blot analysis and quantification of the expression of endogenous TFEB in cystinotic cells are shown. Mean ± S.E. ($n = 3$). *, $p < 0.05$. *C,* exogenous expression of TFEB or TFEB-S3AR4A with constitutive nuclear localization (*N*) increases the perinuclear distribution of LAMP1- (*upper panels*) and LAMP2A (*bottom panels*)-positive organelles in cystinotic cells. Immunofluorescence of endogenous LAMP1 or LAMP2A (*red*) and the cellular distribution of GFP-TFEB or GFP-TFEB-S3AR4A in wild-type (*WT*) or *Ctns*$^{-/-}$ cells was analyzed as described under "Materials and methods." *Scale bars,* 20 μm. *N,* denotes nucleus. *D,* immunofluorescence analysis of endogenous LAMP1 and LAMP2A localization in *Ctns*$^{-/-}$ cells either treated with genistein to activate TFEB or with vehicle (DMSO). Similar to that observed for TFEB overexpression, genistein treatment induces perinuclear localization of LAMP1 in cystinosis. Quantitative analysis indicates that genistein treatment improves the localization of LAMP2A at LAMP1-positive organelles. Mean ± S.E. ($n = 3$). ***, $p < 0.001$.

and LAMP2A (Fig. 7*C*), a phenotype that recapitulates that observed in cells overexpressing RILP and also similar to what occurs when Rab7Q67L is expressed (37). These studies suggest that the transcription factor TFEB regulates lysosomal distribution most likely through the up-regulation of RILP. Next, to analyze whether TFEB up-regulation affects LAMP2A localization, we treated wild-type and cystinotic cells with the natural isoflavone genistein that has a direct effect on TFEB activation (32). Although genistein treatment had no effect on LAMP2A expression (30), it markedly and significantly increased LAMP2A colocalization at LAMP1-positive structures in cystinotic cells (Fig. 7*D*) further supporting our previous study (30) that TFEB up-regulation may be beneficial in cystinosis, likely by the transcriptional up-regulation of trafficking regulatory proteins.

To directly analyze whether the up-regulation of Rab11- or Rab7-dependent vesicular trafficking mechanisms have a positive effect on the re-localization of LAMP2A to LAMP1-positive organelles in cystinosis, we next expressed the constitutively active mutants of these Rab-GTPases, Rab11Q70L and Rab7Q67L, into cystinotic cells and measured LAMP2A/LAMP1 colocalization by immunofluorescence. Remarkably, both Rab11 and Rab7 up-regulations significantly increased the localization of the CMA receptor at lysosomes in *Ctns*$^{-/-}$ cells (Fig. 8, *A* and *B*), further supporting that the trafficking mechanisms are important to up-regulate CMA in these cells. Furthermore, the expression of dominant-negative Rab11 or Rab7 GTPases induced significant impairment in LAMP2A trafficking supporting the idea that Rab11 and Rab7 are necessary for the CMA receptor trafficking. However, these dominant-negative GTPases induced different defective phenotypes, with Rab7-DN but not Rab11-DN affecting granules moving at high speed (Fig. 8*C*). The observations that either Rab11 or Rab7 up-regulation rescues LAMP2A trafficking and localization together with the data showing that dominant-negative Rab11 and Rab7 mutants induced different defective phenotypes (Fig. 8*C*) suggest that these GTPases regulate different trafficking pathways. Of note, neither Rab7-DN nor Rab11-DN induced the accumulation of LAMP2A at the plasma membrane in WT or *Ctns*$^{-/-}$ cells (Fig. 8*D*).

CMA activity is an essential mechanism to maintain cellular homeostasis, and CMA activation is part of the cellular response to oxidative stress. Furthermore, blockage of CMA decreases cellular viability following exposure to different prooxidant compounds (10, 38, 39). We have previously shown that *Ctns*$^{-/-}$ cells have marked up-regulation of the unfolded protein response, ER expansion, and increased susceptibility to oxidative stress (19, 24). Here, we hypothesized that CMA up-regulation may constitute an effective mechanism to restore cellular homeostasis and survival in cystinosis. First, we show that treatment with QX77 corrects the localization of LAMP2A at the lysosomal membrane in cystinotic cells (Fig. 9, *A* and *B*), supporting the idea that CMA activators may correct cell activity in the context of cystinosis, at least in part, by increasing LAMP2A localization at the lysosomal membrane. Of note, the overexpression of CMA-competent LAMP2A, with an untagged C terminus, also partially rescued the defective phenotype (Fig. 9*C*). This is explained by the observation that a small pool of LAMP2A localizes at lysosomes in cystinosis, but it also supports that CMA up-regulation facilitates trafficking. We next questioned whether the up-regulation of CMA by QX77 treatment correlated with repaired cell function and tolerance to stress in cystinosis. To this end, the cells were exposed to the oxidative stressor *t*-butyl hydroperoxide, and cell survival was monitored in cells treated with QX77 or vehicle. We show that QX77 treatment protects cystinotic cells from the increased susceptibility to oxidative stress and reconstitutes the resistant levels observed in wild-type cells (Fig. 9*D*). The effect of QX77 on cystinotic cell survival was dependent on LAMP2A expression as the effect was prevented by LAMP2A knockdown (Fig. 9*E*). These studies support the idea that repairing CMA by small-molecule CMA activators may constitute a potential novel therapeutic approach in cystinosis.

Discussion

Lysosomal localization of LAMP2A is essential for the proper degradation of substrates through chaperone-mediated autophagy. Here, we demonstrate for the first time a mechanism mediated by the lysosomal transmembrane protein CTNS to facilitate LAMP2A trafficking and lysosomal localization (Fig. 10). The function of CTNS as a facilitator of trafficking is independent of its cystine transporter activity, because CTNS point mutants that conserve lysosomal localization but lack cystine transporter activity increase LAMP2A trafficking and distribution at the lysosomal membrane as efficiently as the wild-type protein. We also demonstrate that LAMP2A trafficking is regulated by the small GTPases Rab11 and Rab7, and we identified the Rab7 effector RILP as an additional regulator of this process. Down-regulation of both Rab11 and RILP are features of cystinotic cells, where LAMP2A is accumulated at Rab11-positive carrier vesicles. We found that the up-regulation of Rab11 or Rab7/RILP independently leads to the correction of the LAMP2A-mislocalization phenotype in the cystinotic cells. The regulation of the expression of these GTPases is also independently controlled. Thus, TFEB activation up-regulates RILP expression and rescues the localization of LAMP2A at the lysosomal membrane but does not regulate Rab11 expression. In contrast, up-regulation of CMA through treatment with small molecules that revert a repressive transcriptional mechanism on CMA mediated by the retinoic acid receptor-α (31) up-regulates Rab11 expression, and it corrects Rab11-dependent trafficking and LAMP2A localization but not RILP expression. Importantly, CMA activators improve cellular function and increase survival to oxidative stress-induced cell death in cystinosis, highlighting CMA as a novel therapeutic target for this lysosomal storage disease.

Here, we show that LAMP2A-positive organelles are characterized by impaired trafficking in cystinotic cells. This defect is specific for LAMP2A because LAMP1 localization at the lysosomal membrane is not affected in cystinosis (19) despite the impaired trafficking of both endocytic intermediate vesicles and late endosomes (24) in *Ctns*$^{-/-}$ cells, thus highlighting LAMP2A-specific trafficking defects in this lysosomal storage disorder. After their synthesis in the ER and trafficking through the Golgi, lysosome-associated membrane proteins, and LAMP2A in particular, utilize several pathways to reach

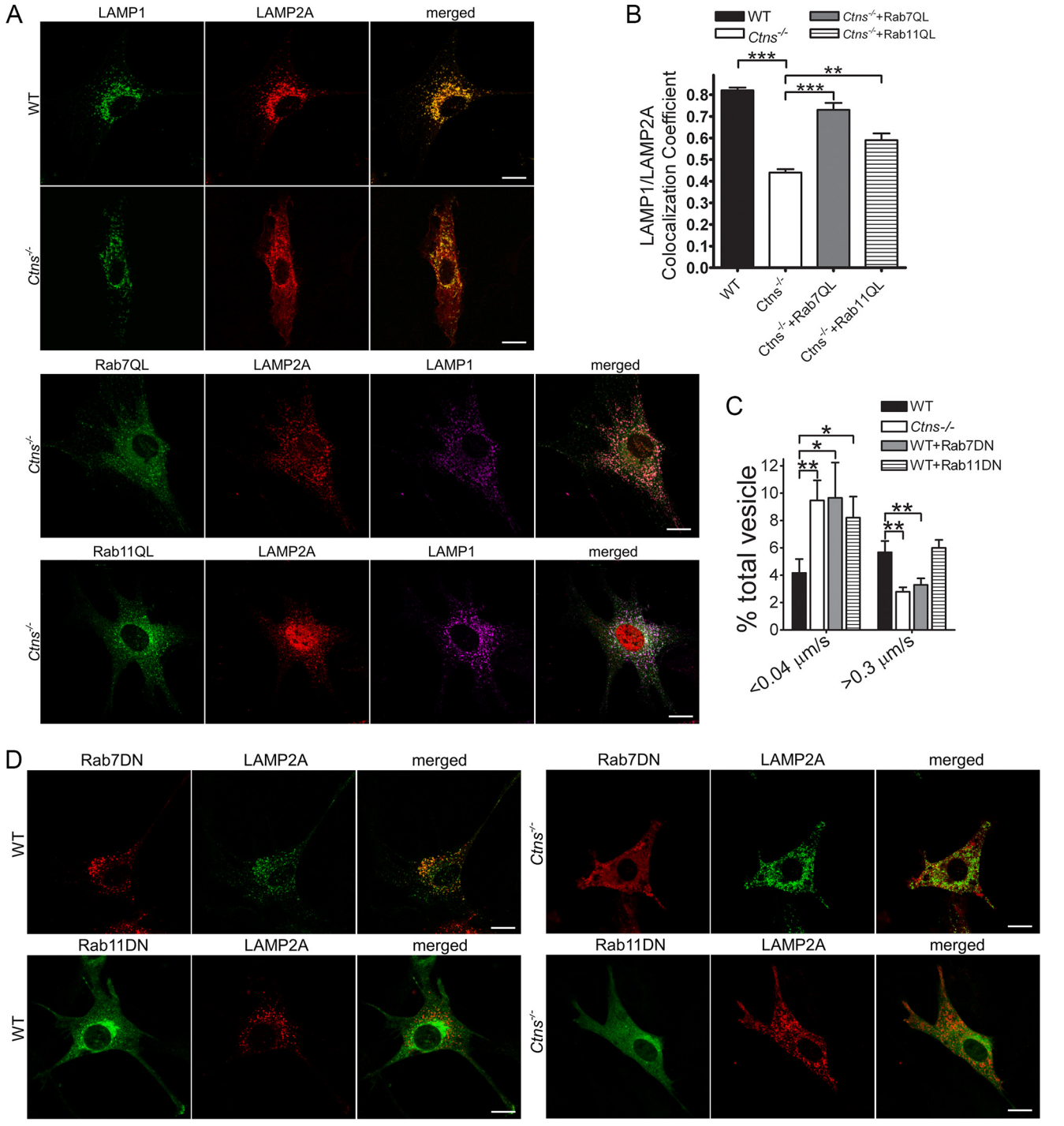

Figure 8. Rab7 and Rab11 independently regulate LAMP2A trafficking. *A,* confocal microscopy analysis of the localization of LAMP1 and LAMP2A in WT and *Ctns*$^{-/-}$ MEFs. WT and *Ctns*$^{-/-}$ MEFs were transfected with Rab7QL or Rab11QL expression vector and immunostained for endogenous LAMP1 and LAMP2A. *Scale bar,* 20 μm. *B,* quantification of the colocalization of LAMP1- and LAMP2A-positive organelles using ImageJ. At least 14 cells from two independent experiments were quantified. Mean ± S.E. **, $p < 0.01$, and ***, $p < 0.001$, Student's *t* test. *C,* effect of Rab11 and Rab7 dominant-negative GTPases on the vesicular trafficking of LAMP2A. WT and *Ctns*$^{-/-}$ MEFs were transfected with GFP- or mCherry-LAMP2A. Where indicated, the WT cells were cotransfected for the expression of DsRed-Rab7-DN or GFP-Rab11-DN. LAMP2A vesicular trafficking was performed by pseudo-TIRFM. *Histograms* representing the speeds of LAMP2A-containing organelles are shown. Results are represented as mean ± S.E. from at least 20 cells. *, $p < 0.05$, Student's *t* test. *D,* representative images showing the localization of endogenous LAMP2A in WT or *Ctns*$^{-/-}$ MEFs expressing DsRed-Rab7-DN or GFP-Rab11-DN and analyzed by confocal microscopy. *Scale bar,* 20 μm.

the lysosome (33, 40, 41). Despite having ER enlargement (24), LAMP2A is not retained in the ER in cystinosis (19). Instead, we found accumulation of LAMP2A at Rab11-positive vesicles, compartments that have decreased motility in the absence of cystinosin expression, thus linking LAMP2A trafficking with Rab11 function. The delivery of lysosomal membrane proteins to the lysosome through the constitutive secretory pathway and subsequent internalization through the endocytic pathway may require rounds of exocytosis and endocytosis before delivery to lysosomes (33, 42). It would be tempting to propose the hypoth-

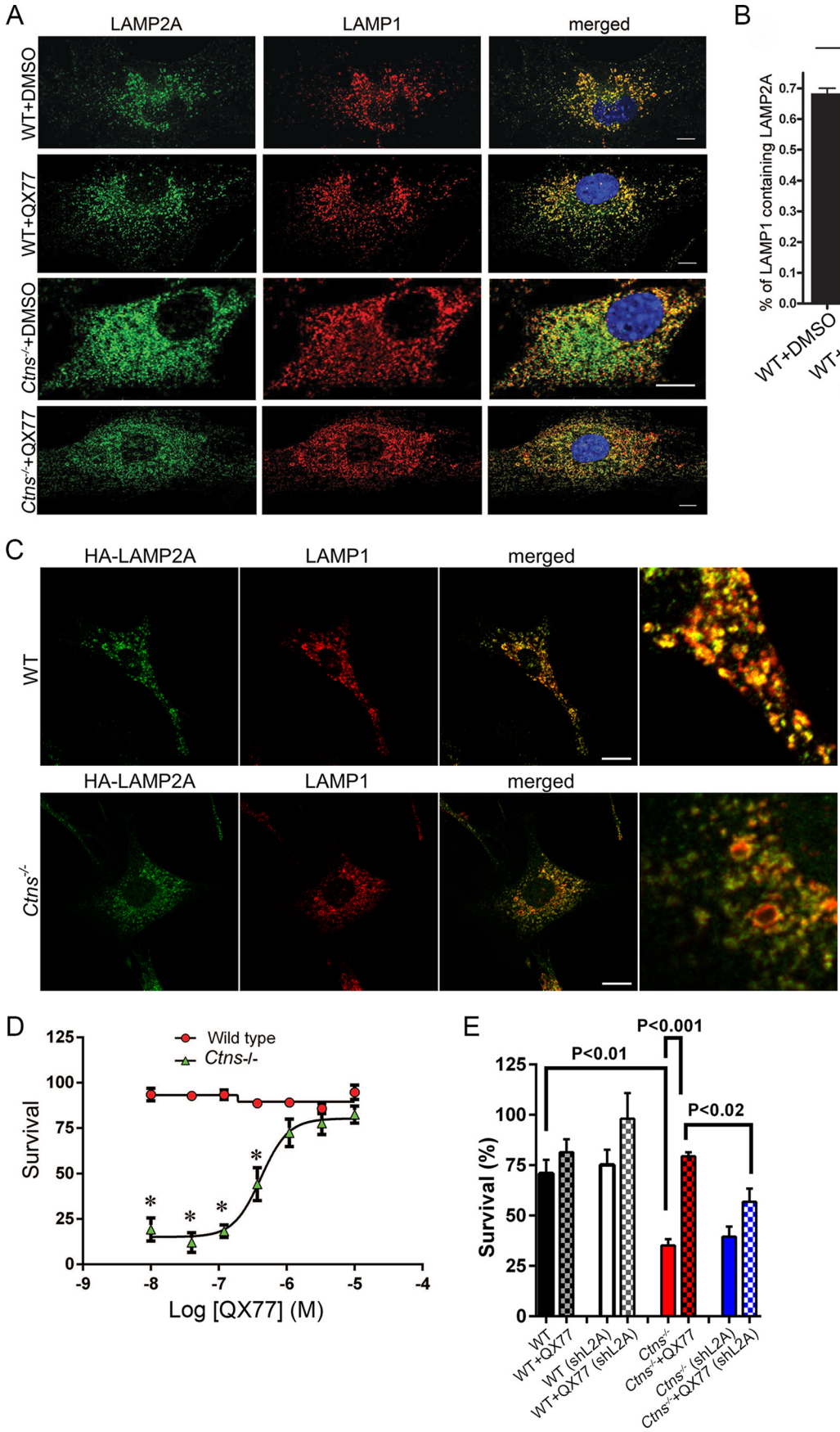
A
LAMP2A
LAMP1
merged
WT+DMSO
WT+QX77
Ctns-/-+DMSO
Ctns-/-+QX77
B
***
***
% of LAMP1 containing LAMP2A
0.0
0.1
0.2
0.3
0.4
0.5
0.6
0.7
WT+DMSO
WT+QX77
Ctns-/-+DMSO
Ctns-/-+QX77
C
HA-LAMP2A
LAMP1
merged
WT
HA-LAMP2A
LAMP1
merged
Ctns-/-
D
Wild type
Ctns-/-
Survival
0
25
50
75
100
125
-9
-8
-7
-6
-5
-4
Log [QX77] (M)
E
P<0.001
P<0.01
P<0.02
Survival (%)
0
25
50
75
100
125
WT
WT+QX77
WT (shL2A)
WT+QX77 (shL2A)
Ctns-/-
Ctns-/-+QX77
Ctns-/- (shL2A)
Ctns-/-+QX77 (shL2A)

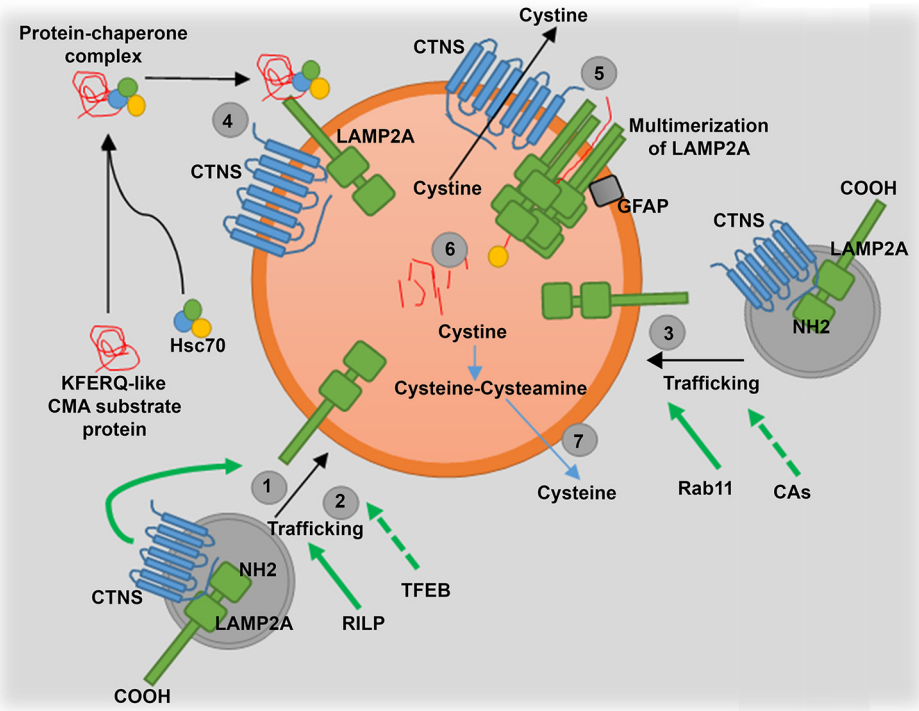

Figure 10. Schematic representation of CTNS regulation of LAMP2A trafficking. CTNS regulates LAMP2A trafficking to lysosomes, and its deficiency causes LAMP2A mislocalization, but the cystine-transporter activity of CTNS is not necessary for LAMP2A trafficking (*1–3*). RILP is down-regulated in cystinosis, and its rescue also up-regulates LAMP2A trafficking (*2*). In addition, TFEB up-regulation increases LAMP2A localization at the lysosomal membrane despite LAMP2A expression being independent of TFEB (*2*). Rab11 is also down-regulated in cystinosis, and this GTPase controls the trafficking of a subpopulation of LAMP2A molecules to the lysosomal membrane (*3*). Treatment with CMA activator (*CA*, QX77) rescues Rab11 down-regulation and trafficking deficiency in cystinotic cells (*3*). QX77 treatment also increases LAMP2A localization at the lysosomal membrane (*4*). As a consequence of LAMP2A mislocalization, the internalization of CMA substrates into lysosomes is defective in CTNS deficiency (*5*). In the absence of CTNS, degradation of CMA substrate is defective (*6*). The mechanism of CMA is not repaired by decreased lysosomal overload induced by cysteamine treatment (*7*).

esis that Rab11, a GTPase frequently associated with recycling endosome trafficking to the plasma membrane, is involved in the recycling of LAMP2A to the plasma membrane before its delivery to the lysosome through the endocytic pathway. However, neither constitutively active nor dominant-negative Rab11 induced accumulation of LAMP2A at the plasma membrane, and no accumulation of LAMP2A at the plasma membrane was observed in Rab11-deficient cystinotic cells, suggesting that Rab11 regulates the direct delivery of LAMP2A to the lysosome, independently of endosome recycling or other indirect pathways. Rab11-FIP4, is a Rab11 effector that operates in cellular events other than endosomal recycling (43) and whose overexpression condenses endogenous Rab11 in the perinuclear area (43), thus resembling lysosomal distribution. Interestingly, we found that Rab11-FIP4 expression is down-regulated in cystinotic kidneys (RNA array, fold change: 0.63; $p < 2.8 \times 10^{-6}$) thus supporting a possible direct delivery of LAMP2A to the lysosome through a Rab11/Rab11-FIP4-dependent pathway in cystinosis.

Similar to Rab11, the expression of Rab7 or RILP rescued the LAMP2A trafficking/localization-defective phenotype in cystinosis, but expression of their dominant negatives did not induce an overt accumulation of LAMP2A at the plasma membrane suggesting similarity between the two GTPases. However, the observations 1) that up-regulation of Rab11 or Rab7 independently increased the re-localization of LAMP2A at the lysosomal membrane, 2) that Rab7 elicited a more significant improvement of the LAMP2A lysosomal localization than Rab11, and 3) that dominant-negative Rab7 affected the trafficking of a sub-population of vesicles that was not impaired by dominant-negative Rab11 suggest that Rab7 regulates trafficking of a subpopulation of LAMP2A-positive vesicles independently of Rab11. The regulation of the delivery of LAMP proteins to the lysosome by alternative transport pathways using luminal or transmembrane determinants has been proposed (34). Based on our studies, we propose Rab11, Rab7, RILP, and CTNS as new molecular determinants of the specific machinery for LAMP2A trafficking to lysosomes.

Figure 9. Small-molecule CMA activators increase LAMP2A relocalization at the lysosomal membrane and survival to oxidative stress-induced cell death in cystinosis. *A* and *B,* confocal microscopy analysis of the colocalization of LAMP2A and LAMP1. *A,* representative images of wild-type (*WT*) or *Ctns*$^{-/-}$ cells treated with the CMA activator (QX77) or vehicle (DMSO). *Scale bar,* 10 μm. *B,* quantitative analysis of protein colocalization showing that QX77 significantly increases the re-localization of LAMP2A at LAMP1-positive lysosomes in cystinotic cells. ***, $p < 0.001$. *C,* localization of a CMA-competent LAMP2A, with an internal HA-tagged but free C terminus, in wild-type and cystinotic cells. *D,* effect of CMA activator (QX77) on cell survival (MTT assay) to 100 μM *tert*-butylhydroperoxide-induced oxidative stress. Results are mean ± S.E. from three biological replicates. Representative of three independent experiments with similar results. *, $p < 0.0015$. *E,* WT and *Ctns*$^{-/-}$ MEFs were infected with lentiviral shRNA against mouse LAMP2A for 7 days. MTT assay was performed as described under "Materials and methods."

Antignac and co-workers (5) demonstrate that the sorting of cystinosin to lysosomes requires two molecular signatures, a classical tyrosine-based sorting signal motif (GYDQL) in the C-terminal tail and a conformational signal delineated to a region of the fifth inter-transmembrane loop. The second sorting signal is not well defined, and a mechanism mediated by the dynamic interaction of cystinosin with another lysosomal protein that possesses a sorting motif through the second signal structure of cystinosin has been proposed (5). Our observations presented here that CTNS rescues LAMP2A trafficking and localization and that CTNS reaches the lysosomal membrane in the absence of LAMP2A suggest that whereas a dynamic interaction between CTNS and LAMP2A may help transport and position LAMP2A at the lysosomal membrane, LAMP2A seems to be dispensable for CTNS trafficking. Thus, our observation that in LAMP2A-knock-out (KO) cells, CTNS traffics and localizes at the lysosomal membrane as efficiently as in wild-type cells, indicates that whereas CTNS affects LAMP2A trafficking, the mechanism is not reciprocal. We also show that CTNS-LKG, a natural isoform of CTNS in which the C-terminal domain, including the targeting sequence GYDQL, is replaced by a longer string of 38 amino acids, rescues LAMP2A localization. These data support the idea that the internal targeting domain and not the C-terminal domain is important for CTNS to mediate LAMP2A localization. The CTNS function as a trafficking modulator of LAMP2A could be explained either by direct interaction of CTNS with LAMP2A to mediate the stabilization of LAMP2A at trafficking intermediate vesicles or by indirect interactions through protein or lipidic mediators. However, direct interaction between CTNS and LAMP2A has not been demonstrated so far, and therefore, it is likely that additional molecules or discrete lysosomal membrane microdomains facilitate the interaction and co-trafficking of these two molecules to the lysosomal membrane.

Although most genetic mutations associated with infantile cystinosis are characterized by a CTNS product with abolished cystine-transporter activity, some discrepancies have been described in which patients with a CTNS protein with negligible transporter activity have a milder manifestation of the disease (5). In particular, a missense mutation in the conserved amino acid Lys-280 generates a CTNS protein with abolished cystine transporter activity that is nonetheless associated with a mild clinical phenotype of juvenile cystinosis (5). The observation that this particular mutant localizes at the lysosomal membrane and restores LAMP2A trafficking and localization at the lysosomes strongly indicates that CTNS has significant functions independently of its role as the only known cystine transporter. We propose that the ability of the $CTNS^{K280R}$ mutant to rescue the localization of the CMA receptor LAMP2A is at least in part responsible for the association of this mutant with a relatively mild juvenile cystinosis phenotype, despite its inability to decrease lysosomal cystine overload.

Despite the efficiency of cysteamine in retarding the rate of tissue deterioration (2, 44), cell malfunction and progressive tissue injury occur regardless of cystine depletion therapy (3), suggesting that cystine accumulation is not the only cause of all the defects in cystinosis (3, 4). We showed that impaired CMA due to aberrant LAMP2A expression and localization is an important pathogenic factor independent of lysosomal overload in cystinosis, stressing the need for additional treatments to cystine-depletion therapies (19). Importantly, cystinotic cells are susceptible to oxidative stress-induced cell death, and CMA activation is part of the cellular response to oxidative stress because blockage of CMA decreases cellular viability following exposure to different pro-oxidant compounds (10, 29, 38, 39). Here, to demonstrate that up-regulation of CMA improves cellular function in cystinosis, we treated cystinotic cells with a CMA activator (QX77), which operates through the release of the endogenous inhibition of the retinoic receptor-α signaling pathway over the regulation of multiple mechanisms that modulate CMA (31). Cystinotic cells treated with QX77 showed a rapid and significant improvement in cell function under oxidative conditions in a dose-response manner, further supporting the idea that CMA enhancement has the potential to improve cellular and tissue function in cystinosis.

The observations that LAMP2A trafficking and localization are impaired in cystinosis, and that treatment with CMA enhancers significantly correct LAMP2A localization, support the idea that improved LAMP2A trafficking induced by up-regulation of the CMA transcriptional machinery regulated by CMA activators improve cellular function in cystinosis at least in part by efficiently re-localizing LAMP2A to the lysosomal membrane. The effect of CMA activators was achieved in the absence of cystinosin expression despite the involvement of CTNS in LAMP2A trafficking. These data suggest that these small molecules operate by up-regulating trafficking mechanisms that can compensate, at least partially, for the absence of CTNS. These mechanisms include the up-regulation of Rab11 expression and perhaps also its effectors. Furthermore, because the effect of CMA activators is LAMP2A-dependent, our data indicate that enhanced trafficking is favored by up-regulation of CMA activity not only by increasing LAMP2A availability (31) but also likely by favoring the degradation of oxidized Rab GTPases and effectors that may be CMA substrates themselves. This would favor the stabilization of Rab GTPases through the interaction with newly synthesized Rab effectors. The overexpression of CMA-competent LAMP2A would also favor this mechanism.

In conclusion, vesicular transport and in particular the trafficking of the CMA receptor LAMP2A emerges as a central regulatory pathway necessary to maintain cellular homeostasis in cystinosis.

Altogether, our data have elucidated a mechanism of LAMP2A translocation in cystinosis that is dependent on CTNS function but is independent of its cystine transporter activity. In addition, we demonstrate that LAMP2A trafficking is regulated by Rab11, and RILP, two molecules previously associated with endosomal and lysosomal transport mechanisms and shown here for the first time to be down-regulated in cystinosis. Finally, we propose the idea that functional CMA would attenuate the clinical manifestations in patients with cystinosis. We also propose that the use of CMA enhancers would repair underlying CMA defects in tissues with cystinosis, a mechanism that is not restored by currently used lysosomal depletion therapies.

Materials and methods

Animal models

All animal studies were performed in compliance with the United States Department of Health and Human Services Guide for the Care and Use of Laboratory Animals. All studies were conducted according to National Institutes of Health and institutional guidelines and with approval of the animal review boards at The Scripps Research Institute and University of California, San Diego. The C57BL/6 *Ctns*$^{-/-}$ mice were described before (45). For CMA activity, C57BL/6 wild-type and C57BL/6 *Ctns*$^{-/-}$ mice were between 8 and 12 weeks old. Neonatal skin fibroblasts from *Ctns*$^{-/-}$ and wild-type mice were prepared by standard procedures (24). The cells were maintained in Dulbecco's modified Eagle's medium (Gibco) supplemented with 10% FBS (Corning Cellgro) and penicillin/streptomycin/glutamine (Life Sciences).

Lysosome fractionation and β-hexosaminidase assay

The purification of the lysosomal fractions for CMA assays was performed as we described previously (19). Briefly, WT and *Ctns*$^{-/-}$ mice were starved for 24 h; livers were collected, homogenized in Tris-buffered 0.25 M sucrose (pH 7.4) in the absence of protease inhibitors, and centrifuged at 6,800 × *g* for 15 min at 4 °C. After washing the pellet with 0.25 M sucrose, the combined supernatants were centrifuged at 17,000 × *g* 20 min at 4 °C. The pellet, which contained the light mitochondria and lysosomal fraction, was then resuspended in 0.25 M sucrose, and mitochondria were precipitated by incubation with 115 μM $CaCl_2$ for 30 min. The supernatants were then centrifuged at 5,000 × *g* for 10 min at 4 °C to pellet the mitochondria. The supernatant, which contains the lysosomes, was collected and centrifuged again at 5,000 × *g* for 10 min at 4 °C to ensure purity. The supernatant was retained and centrifuged at 17,000 × *g* for 20 min at 4 °C to pellet the lysosomes. The lysosomes were then resuspended in reaction buffer (10 mM MOPS (pH 7.3), 0.25 M sucrose, 5.4 μM cysteine, 1 mM DTT). Lysosomal integrity was verified by comparative analysis of β-hexosaminidase activity for intact lysosomes or 1% Triton X-100-lysed lysosomes (19). β-Hexosaminidase activity was measured using the membrane-impermeant fluorogenic substrate 4-methylumbelliferyl-*N*-acetyl-β-glucosaminide dehydrate (Sigma M2133) as described previously (5). Only lysosomes with an integrity of >85% were used in subsequent assays.

CMA assay

CMA assays were performed as described before (19). Briefly, 25 μg of purified lysosomes were incubated for 30 min at 37 °C with 2 μg of purified recombinant GAPDH (Sigma), 10 μl of "6× energy-regenerating system" (60 mM $MgCl_2$, 60 mM ATP, 12 mM phosphocreatine, 30 μg of creatine phosphokinase, in 0.25 M sucrose (pH 7.4)), 0.6 μg of Hsc70 (Enzo Life Science) and brought up to 60 μl with reaction buffer (10 mM MOPS (pH 7.3), 0.25 M sucrose, 5.4 μM cysteine, 1 mM DTT). Control conditions were run in parallel with either no lysosomes, no energy-regenerating system, or by addition of EDTA/protease inhibitor mixture (Roche Applied Science). After incubation at 37 °C for 30 min, a fraction (15%) of the CMA reactions was mixed with sample buffer and boiled at 95 °C for 5 min, followed by SDS-PAGE and GAPDH immunoblotting. For substrate translocation assays, the reactions were spun down to separate lysosomes from their supernatants, and 35% of the lysosomal fraction was analyzed by immunoblotting as described above.

Constructs, transfections, and transductions

The following vectors were purchased from Addgene: TFEB-EGFP, TFEB-EGFP-δ30, TFEB-EGFP-S3AR4A (35), DsRed-Rab7-DN, and GFP-Rab11-DN. The RILP expression vectors (37), GFP-Rab11, GFP-Rab11QL, and GFP-Rab7QL were described before (46). The expression vector for LAMP2A-mCherry was a gift from Dr. Santiago Di Pietro and was described before (27). The pCCL plasmid for lentiviral expression of GFP-CTNS was described previously (19). Lentiviruses expressing GFP-CTNS, GFP-CTNSK280R, and GFP-CTNS-LKG were described before (47). Lentiviral mouse LAMP2A shRNA was described before (48). The transduction of lentiviral vectors in *Ctns*$^{-/-}$ and wild-type cells was performed as described (19).

Gel electrophoresis and immunoblotting

Cells were lysed in lysis buffer containing 20 mM Tris (pH 7.4), 150 mM NaCl, and 1% Triton X-100 in the presence of protease/inhibitor (Roche Applied Science) and phosphatase/inhibitor (Calbiochem) mixtures. Following electrophoresis using 4–12% gradient gels (Life Sciences), proteins were transferred onto 0.45-μm nitrocellulose membranes, and the membranes were incubated overnight in the indicated primary antibodies and then incubated with HRP-conjugated secondary antibodies. The blots were developed using SuperSignal West Pico, Dura, or Femto chemiluminescence substrate systems (Thermo Fisher Scientific). Transferred proteins were visualized using Hyperfilm (Amersham Bioscience). The following antibodies were used for immunoblotting in this study: rat anti-LAMP1 (Santa Cruz Biotechnology, sc-19992); rabbit anti-LAMP2A (Abcam, ab18528) for immunofluorescence; rabbit LAMP2A (Thermo Fisher Scientific, 51-2200) for Western blotting; rabbit anti-actin (Sigma, A2066); rabbit anti-GAPDH (Gene Tex); goat anti-RILP (Santa Cruz Biotechnology, sc-82746); rabbit anti-Rab7 (Cell Signaling, 9367); rat anti-tubulin (Millipore, MAB1864); goat anti-LAMP1 (R&D Systems, AF4320); rabbit anti-TFEB (Bethyl, A303-673A); and mouse anti-KDEL (Enzo Life Sciences, ADI-SPA-827).

Immunofluorescence, immunohistochemistry, and confocal analysis

Wild-type and *Ctns*$^{-/-}$ cells were seeded on untreated number 1.5 borosilicate coverglass (Corning). Where indicated cells were starved as described above, then fixed with 4% paraformaldehyde, and blocked with 1% BSA in PBS in the presence of 0.01% saponin. Samples were labeled with the indicated primary antibodies overnight at 4 °C in the presence of 0.01% saponin and 1% BSA. Samples were washed and subsequently incubated with the appropriate combinations of Alexa Fluor (488, 568, 594, or 647)-conjugated donkey anti-

rabbit, anti-rat, or anti-mouse secondary antibodies (Life Sciences).

For immunofluorescence staining, samples were incubated in blocking buffer (1% bovine serum albumin (BSA), 0.01% saponin, PBS) for 1 h. The samples were incubated with primary antibodies overnight at 4 °C, washed with PBS, and labeled with Alexa Fluor-conjugated secondary antibodies. Nuclei were stained with 4′,6′-diamidino-2-phenylindole (DAPI), and samples were preserved in Fluoromount-G reagent (Southern Biotech) and kept at 4 °C until analyzed. For tissue immunofluorescence, mouse kidneys were fixed in Z-Fix (Anatech Ltd.) for 24 h and immediately processed with a tissue processor, embedded in paraffin, cut with a microtome at 3 μm, and mounted on slides. Dewaxing and antigen retrieval was performed by standard procedures, and staining was performed as described above. Samples were analyzed with a Zeiss LSM 710 laser-scanning confocal microscope attached to a Zeiss Observer Z1 microscope at 21 °C, using a ×63 oil Plan Apo, 1.4-numerical aperture objective. Images were collected using ZEN-LSM software and processed using ImageJ and Adobe Photoshop CS4. Analysis and quantification of protein colocalization were achieved by ImagePro software. The following primary antibodies were used for immunofluorescence in this study: rat anti-LAMP1 (1D4B, Santa Cruz Biotechnology); goat anti-mLAMP1 (AF4320 R&D Systems); rabbit anti-LAMP2A (9); goat anti-megalin (sc16478, Santa Cruz Biotechnology); and anti-GAPDH (GeneTex GTX627408).

Super-resolution microscopy

STORM samples were prepared by labeling cells with anti-LAMP1 1D4B, Santa Cruz Biotechnology, and rabbit anti-LAMP2A (15-amino acid cytosolic tail) (11), primary antibodies, and Alexa Fluor-647 anti-rat and Alexa Fluor-488 anti-rabbit secondary antibodies. Samples were suspended in freshly prepared STORM buffer (50 mM Tris (pH 8.0), 10 mM NaCl, 10% glucose, 0.1 M mercaptoethanolamine (cysteamine; Sigma), 56 units/ml glucose oxidase (from *Aspergillus niger*, Sigma), and 340 units/ml catalase (from bovine liver, Sigma)) and imaged on a Nikon Ti super-resolution microscope. Samples were imaged using a ×100 1.49 NA Apo TIRF objective either with or without TIRF illumination. Images were collected on an ANDOR IXON3 Ultra DU897 EMCCD camera using the multicolor continuous mode setting in the Nikon Elements software. Power on the 488- and 647-nm lasers was adjusted to enable collection of between 50 and 300 molecules per 256 × 256 camera pixel frame at appropriate threshold settings for each channel. Collection was stopped after a sufficient number of frames were collected (usually yielding 1–2 million molecules), and the super-resolution images were reconstructed with the Nikon STORM software. Positions of individual molecules have been localized with high accuracy by switching them on and off sequentially using the 488- and 647-nm lasers at appropriate power settings. The positions determined from multiple switching cycles can show a substantial drift over the duration of the acquisition. This error is considerably reduced by calculating and correcting for sample drift over the course of the experiment by an auto-correlation method used by the Nikon software. This is done by correlating STORM images reconstructed from subsets of localizations at different time segments to that from the beginning of the acquisition (49). Axial drift over the course of the acquisition is minimized by engaging the Nikon perfect focus system. The precision of the localization during a switching cycle is calculated using the Nikon software from the point spread function and the photon count using molecules that are well separated in the sample itself, as well as Alexa Fluor 488- and Alexa Fluor 647-labeled IgG molecules spread on coverslips, and the values (21 nm for Alexa Fluor 488 and 18 nm for Alexa Fluor 647) are in agreement with those reported previously (49, 50). A Gaussian fit was used to localize the position of each event to the final super-resolution image. For super-resolution studies on the distributions of sparsely distributed molecules as those presented in this study, the Nyquist resolution is not necessarily relevant, because the molecular structure itself does not allow a high labeling density (51). High resolution images, fully calibrated, were imported into Imaris, and the images were analyzed and quantified as described before using Imaris (Bitplane Inc.) (46).

TIRF microscopy

TIRF microscopy experiments were performed using a ×100 1.45 numerical aperture TIRF objective (Nikon) on a Nikon TE2000U microscope custom-modified with a TIRF illumination module as described (25). Images were acquired on a 14-bit cooled charge-coupled device camera (Hamamatsu) controlled through NIS-Elements software. For live experiments, the images were recorded using 300–500-ms exposures depending on the fluorescence intensity of the sample. The images were then analyzed using Imaris as described before (52).

Analysis of cell survival to oxidative stress

Metabolic activity was determined by the MTT assays as described before (53). MRFs were seeded onto 96-well plates at 20,000 cells/well and grown for 24 h. The following day, MEFs were replenished with fresh culture medium containing 10% dialyzed FBS and preincubated with QX77 or vehicle (DMSO) 48 h before the addition of *tert*-butyl hydroperoxide. This chemical oxidant was added at concentrations that had been found to kill more than 80–90% of the *Ctns*$^{-/-}$ cells in previous dose-response assays. After an overnight incubation, cell viability was determined by a modified version of the MTT assay (53). The assay was performed by removing the cell culture medium and replacing it with 100 μl of fresh culture medium containing 5.0 mg/ml MTT. After 4 h of incubation at 37 °C, cells were solubilized overnight with 100 μl of a solution containing 50% dimethylformamide and 20% SDS (pH 4.7). The absorbance at 560 nm was measured with a microplate reader (Spectromax 190; Molecular Devices Corp., Sunnyvale, CA). To ensure that the spectrophotometric readings correlated with cell viability, all cells were examined by microscopy before the addition of the MTT. Each experiment was performed at least three times. For each concentration of a specific compound, three wells were analyzed. Background absorbance values consisted of blank wells (with no cells) into which medium, MTT dye, and solubilization buffer were added. The background readings were subtracted from the average absorbance readings of the treated

wells to obtain an adjusted absorbance reading that represented cell viability. This reading was divided by the adjusted absorbance reading of untreated cells in control wells to obtain the percentage of cell survival. To determine the efficacy, potency, and EC_{50} values of the compounds of interest, the dose-response data were analyzed (Prism 4 software; GraphPad, San Diego).

Gene expression microarray analysis

Sixteen-month-old C57BL/6 wild-type ($n = 6$) and *Ctns*$^{-/-}$ ($n = 6$) mice were euthanized, and their liver, muscle, spleen, and kidney were immediately removed and stored at −80 °C in RNA Later (Life Technologies, Inc.). Tissues were subsequently ground using Precellys 24 (Bertin Technologies, Rockville, MD), and RNA was isolated using the Qiagen AllPrep DNA/RNA Mini kit (Qiagen, Valencia, CA). The RNA was run on a Bioanalyzer (Agilent, Santa Clara, CA) for quantification and quality assessment. The Ambion WT expression kit was used to generate double-stranded biotinylated cDNA, and the Affymetrix HT WT terminal labeling kit was used to prepare the cDNA for hybridization to Affymetrix GeneChip Mouse Gene 1.1 ST arrays (Affymetrix, Santa Clara, CA). The data were collected as CEL files, and quality control analysis was performed with the Affymetrix Expression Console. Normalized signal intensities were generated with Robust Multichip Average, which employs a background adjustment and quantile normalization strategy. Genes without an average $\log_2$-transformed signal above 6 in either the wild-type or *Ctns*$^{-/-}$ group were removed from further analysis. Class comparisons of variance by two-way *t* tests for two sample comparisons ($p < 0.001$) were performed using BRB-ArrayTools (http://linus.nci.nih.gov/BRB-ArrayTools) to identify the set of significantly differentially expressed genes between wild-type and *Ctns*$^{-/-}$ mice in each tissue.

qRT-PCR

Quantitative RT-PCR RNA was isolated from wild-type or *Ctns*$^{-/-}$ mouse fibroblasts using the RNeasy mini-kit for RNA purification (Qiagen), which includes gDNA-eliminator columns. A total of 100 ng of RNA for each cell line was reverse-transcribed (RT) using iScript cDNA synthesis kit (Bio-Rad). Quantitative RT-PCR was performed using QuantiTect SYBR Green PCR mix (Qiagen), with the following primer mixes: mouse RILP, RILP-qPCR forward, TTCCAGCGAGAGCTGCTCAC, and RILP-qPCR reverse, CATCCTCACTGCTCTCTGC; mouse β-actin forward, CATTGTTACCAACTGGGACG, and mouse β-actin reverse, CAGAGGCATACAGGGACAG.

Statistical analysis

Data are presented as means, and error bars correspond to standard errors of the means (S.E.), unless otherwise indicated. Statistical significance was determined using the unpaired Student's *t* test using GraphPad InStat (version 3) or GraphPad Prism (version 6) software, and graphs were made using GraphPad Prism (version 6) software. *p* values <0.05 were considered statistically significant.

Author contributions—J. Z. performed experiments, analyzed data, contributed ideas and comments, and contributed to manuscript writing; J. L. J. and J. H. performed experiments, analyzed data, and contributed ideas and comments; G. N. performed experiments, analyzed data, and contributed ideas and comments; M. R. and C. R. contributed ideas and comments; W. B. K. performed experiments and analyzed data; C. B. contributed important reagents; E. G. and Q. X. designed/validated QX77 and contributed reagents; A. M. C. designed/validated QX77, contributed reagents, ideas, and comments; S. C. contributed reagents, ideas, and comments; S. D. C. conceived the idea, designed the manuscript and the experimental approach, performed experiments, analyzed data, and wrote the manuscript with input from J. Z. and J. L. J.

Acknowledgments—We thank Drs. Corinne Antignac and Santiago Di Pietro for the contribution of reagents. We also thank Dr. Kersi Pestonjamasp for help with STORM.

References

1. Town, M., Jean, G., Cherqui, S., Attard, M., Forestier, L., Whitmore, S. A., Callen, D. F., Gribouval, O., Broyer, M., Bates, G. P., van't Hoff, W., and Antignac, C. (1998) A novel gene encoding an integral membrane protein is mutated in nephropathic cystinosis. *Nat. Genet.* **18,** 319–324
2. Gahl, W. A., Thoene, J. G., and Schneider, J. A. (2002) Cystinosis. *N. Engl. J. Med.* **347,** 111–121
3. Cherqui, S. (2012) Cysteamine therapy: a treatment for cystinosis, not a cure. *Kidney Int.* **81,** 127–129
4. Vaisbich, M. H., Pache de Faria Guimaraes, L., Shimizu, M. H., and Seguro, A. C. (2011) Oxidative stress in cystinosis patients. *Nephron Extra* **1,** 73–77
5. Kalatzis, V., Nevo, N., Cherqui, S., Gasnier, B., and Antignac, C. (2004) Molecular pathogenesis of cystinosis: effect of CTNS mutations on the transport activity and subcellular localization of cystinosin. *Hum. Mol. Genet.* **13,** 1361–1371
6. Klionsky, D. (2007) Autophagy: from phenomenology to molecular understanding in less than a decade. *Nat. Rev. Mol. Cell Biol.* **8,** 931–937
7. Kroemer, G., Mariño, G., and Levine, B. (2010) Autophagy and the integrated stress response. *Mol. Cell* **40,** 280–293
8. Kaushik, S., and Cuervo, A. (2012) Chaperone-mediated autophagy: a unique way to enter the lysosome world. *Trends Cell Biol.* **22,** 407–417
9. Cuervo, A. M., and Dice, J. F. (2000) Unique properties of lamp2a compared to other lamp2 isoforms. *J. Cell Sci.* **113,** 4441–4450
10. Massey, A. C., Kaushik, S., Sovak, G., Kiffin, R., and Cuervo, A. M. (2006) Consequences of the selective blockage of chaperone-mediated autophagy. *Proc. Natl. Acad. Sci. U.S.A.* **103,** 5805–5810
11. Cuervo, A. M., and Dice, J. F. (1996) A receptor for the selective uptake and degradation of proteins by lysosomes. *Science* **273,** 501–503
12. Cuervo, A. M., and Dice, J. F. (2000) Regulation of lamp2a levels in the lysosomal membrane. *Traffic* **1,** 570–583
13. Wilmer, M. J., Emma, F., and Levtchenko, E. N. (2010) The pathogenesis of cystinosis: mechanisms beyond cystine accumulation. *Am. J. Physiol. Renal Physiol.* **299,** F905–F916
14. Galarreta, C. I., Forbes, M. S., Thornhill, B. A., Antignac, C., Gubler, M. C., Nevo, N., Murphy, M. P., and Chevalier, R. L. (2015) The swan-neck lesion: proximal tubular adaptation to oxidative stress in nephropathic cystinosis. *Am. J. Physiol. Renal Physiol.* **308,** F1155–F1166
15. Cuervo, A. M., Hildebrand, H., Bomhard, E. M., and Dice, J. F. (1999) Direct lysosomal uptake of α2-microglobulin contributes to chemically induced nephropathy. *Kidney Int.* **55,** 529–545
16. Sooparb, S., Price, S. R., Shaoguang, J., and Franch, H. A. (2004) Suppression of chaperone-mediated autophagy in the renal cortex during acute diabetes mellitus. *Kidney Int.* **65,** 2135–2144
17. Cuervo, A. (2010) Chaperone-mediated autophagy: selectivity pays off. *Trends Endocrinol. Metab.* **21,** 142–150

18. Li, W., Yang, Q., and Mao, Z. (2011) Chaperone-mediated autophagy: machinery, regulation and biological consequences. *Cell. Mol. Life Sci.* **68,** 749–763
19. Napolitano, G., Johnson, J. L., He, J., Rocca, C. J., Monfregola, J., Pestonjamasp, K., Cherqui, S., and Catz, S. D. (2015) Impairment of chaperone-mediated autophagy leads to selective lysosomal degradation defects in the lysosomal storage disease cystinosis. *EMBO Mol. Med.* **7,** 158–174
20. Kaushik, S., Bandyopadhyay, U., Sridhar, S., Kiffin, R., Martinez-Vicente, M., Kon, M., Orenstein, S. J., Wong, E., and Cuervo, A. M. (2011) Chaperone-mediated autophagy at a glance. *J. Cell Sci.* **124,** 495–499
21. Kaushik, S., and Cuervo, A. (2008) Chaperone-mediated autophagy. *Methods Mol. Biol.* **445,** 227–244
22. Taranta, A., Petrini, S., Palma, A., Mannucci, L., Wilmer, M. J., De Luca, V., Diomedi-Camassei, F., Corallini, S., Bellomo, F., van den Heuvel, L. P., Levtchenko, E. N., and Emma, F. (2008) Identification and subcellular localization of a new cystinosin isoform. *Am. J. Physiol. Renal Physiol.* **294,** F1101–F1108
23. Taranta, A., Petrini, S., Citti, A., Boldrini, R., Corallini, S., Bellomo, F., Levtchenko, E., and Emma, F. (2012) Distribution of cystinosin-LKG in human tissues. *Histochem. Cell Biol.* **138,** 351–363
24. Johnson, J. L., Napolitano, G., Monfregola, J., Rocca, C. J., Cherqui, S., and Catz, S. D. (2013) Upregulation of the Rab27a-dependent trafficking and secretory mechanisms improves lysosomal transport, alleviates endoplasmic reticulum stress, and reduces lysosome overload in cystinosis. *Mol. Cell. Biol.* **33,** 2950–2962
25. Johnson, J. L., Monfregola, J., Napolitano, G., Kiosses, W. B., and Catz, S. D. (2012) Vesicular trafficking through cortical actin during exocytosis is regulated by the Rab27a effector JFC1/Slp1 and the RhoA-GTPase-activating protein Gem-interacting protein. *Mol. Biol. Cell* **23,** 1902–1916
26. Mudrakola, H. V., Zhang, K., and Cui, B. (2009) Optically resolving individual microtubules in live axons. *Structure* **17,** 1433–1441
27. Ambrosio, A. L., Boyle, J. A., and Di Pietro, S. M. (2012) Mechanism of platelet dense granule biogenesis: study of cargo transport and function of Rab32 and Rab38 in a model system. *Blood* **120,** 4072–4081
28. Schneider, J. L., Suh, Y., and Cuervo, A. M. (2014) Deficient chaperone-mediated autophagy in liver leads to metabolic dysregulation. *Cell Metab.* **20,** 417–432
29. Schneider, J. L., Villarroya, J., Diaz-Carretero, A., Patel, B., Urbanska, A. M., Thi, M. M., Villarroya, F., Santambrogio, L., and Cuervo, A. M. (2015) Loss of hepatic chaperone-mediated autophagy accelerates proteostasis failure in aging. *Aging Cell* **14,** 249–264
30. Rega, L. R., Polishchuk, E., Montefusco, S., Napolitano, G., Tozzi, G., Zhang, J., Bellomo, F., Taranta, A., Pastore, A., Polishchuk, R., Piemonte, F., Medina, D. L., Catz, S. D., Ballabio, A., and Emma, F. (2016) Activation of the transcription factor EB rescues lysosomal abnormalities in cystinotic kidney cells. *Kidney Int.* **89,** 862–873
31. Anguiano, J., Garner, T. P., Mahalingam, M., Das, B. C., Gavathiotis, E., and Cuervo, A. M. (2013) Chemical modulation of chaperone-mediated autophagy by retinoic acid derivatives. *Nat. Chem. Biol.* **9,** 374–382
32. Moskot, M., Montefusco, S., Jakóbkiewicz-Banecka, J., Mozolewski, P., Wegrzyn, A. Di Bernardo, D., Węgrzyn, G., Medina, D. L., Ballabio, A., and Gabig-Cimińska, M. (2014) The phytoestrogen genistein modulates lysosomal metabolism and transcription factor EB (TFEB) activation. *J. Biol. Chem.* **289,** 17054–17069
33. Gough, N. R., and Fambrough, D. M. (1997) Different steady state subcellular distributions of the three splice variants of lysosome-associated membrane protein LAMP-2 are determined largely by the COOH-terminal amino acid residue. *J. Cell Biol.* **137,** 1161–1169
34. Janvier, K., and Bonifacino, J. S. (2005) Role of the endocytic machinery in the sorting of lysosome-associated membrane proteins. *Mol. Biol. Cell* **16,** 4231–4242
35. Roczniak-Ferguson, A., Petit, C. S., Froehlich, F., Qian, S., Ky, J., Angarola, B., Walther, T. C., and Ferguson, S. M. (2012) The transcription factor TFEB links mTORC1 signaling to transcriptional control of lysosome homeostasis. *Sci. Signal.* **5,** ra42
36. Martina, J. A., and Puertollano, R. (2013) Rag GTPases mediate amino acid-dependent recruitment of TFEB and MITF to lysosomes. *J. Cell Biol.* **200,** 475–491
37. Cantalupo, G., Alifano, P., Roberti, V., Bruni, C. B., and Bucci, C. (2001) Rab-interacting lysosomal protein (RILP): the Rab7 effector required for transport to lysosomes. *EMBO J.* **20,** 683–693
38. Kiffin, R., Christian, C., Knecht, E., and Cuervo, A. M. (2004) Activation of chaperone-mediated autophagy during oxidative stress. *Mol. Biol. Cell* **15,** 4829–4840
39. Massey, A. C., Zhang, C., and Cuervo, A. M. (2006) Chaperone-mediated autophagy in aging and disease. *Curr. Top. Dev. Biol.* **73,** 205–235
40. Karlsson, K., and Carlsson, S. R. (1998) Sorting of lysosomal membrane glycoproteins lamp-1 and lamp-2 into vesicles distinct from mannose 6-phosphate receptor/γ-adaptin vesicles at the trans-Golgi network. *J. Biol. Chem.* **273,** 18966–18973
41. Akasaki, K., Michihara, A., Fujiwara, Y., Mibuka, K., and Tsuji, H. (1996) Biosynthetic transport of a major lysosome-associated membrane glycoprotein 2, lamp-2: a significant fraction of newly synthesized lamp-2 is delivered to lysosomes by way of early endosomes. *J. Biochem.* **120,** 1088–1094
42. Lippincott-Schwartz, J., and Fambrough, D. M. (1986) Lysosomal membrane dynamics: structure and interorganellar movement of a major lysosomal membrane glycoprotein. *J. Cell Biol.* **102,** 1593–1605
43. Wallace, D. M., Lindsay, A. J., Hendrick, A. G., and McCaffrey, M. W. (2002) Rab11-FIP4 interacts with Rab11 in a GTP-dependent manner and its overexpression condenses the Rab11 positive compartment in HeLa cells. *Biochem. Biophys. Res. Commun.* **299,** 770–779
44. da Silva, V. A., Zurbrügg, R. P., Lavanchy, P., Blumberg, A., Suter, H., Wyss, S. R., Lüthy, C. M., and Oetliker, O. H. (1985) Long-term treatment of infantile nephropathic cystinosis with cysteamine. *N. Engl. J. Med.* **313,** 1460–1463
45. Nevo, N., Chol, M., Bailleux, A., Kalatzis, V., Morisset, L., Devuyst, O., Gubler, M. C., and Antignac, C. (2010) Renal phenotype of the cystinosis mouse model is dependent upon genetic background. *Nephrol. Dial. Transplant.* **25,** 1059–1066
46. Johnson, J. L., He, J., Ramadass, M., Pestonjamasp, K., Kiosses, W. B., Zhang, J., and Catz, S. D. (2016) Munc13-4 is a Rab11-binding protein that regulates Rab11-positive vesicle trafficking and docking at the plasma membrane. *J. Biol. Chem.* **291,** 3423–3438
47. Harrison, F., Yeagy, B. A., Rocca, C. J., Kohn, D. B., Salomon, D. R., and Cherqui, S. (2013) Hematopoietic stem cell gene therapy for the multisystemic lysosomal storage disorder cystinosis. *Mol. Ther.* **21,** 433–444
48. Kon, M., Kiffin, R., Koga, H., Chapochnick, J., Macian, F., Varticovski, L., and Cuervo, A. M. (2011) Chaperone-mediated autophagy is required for tumor growth. *Sci. Transl. Med.* **3,** 109ra117
49. Huang, B., Wang, W., Bates, M., and Zhuang, X. (2008) Three-dimensional super-resolution imaging by stochastic optical reconstruction microscopy. *Science* **319,** 810–813
50. Rust, M. J., Bates, M., and Zhuang, X. (2006) Sub-diffraction-limit imaging by stochastic optical reconstruction microscopy (STORM). *Nat. Methods* **3,** 793–795
51. Xu, K., Shim, S. H., and Zhuang, X. (2013) in *Far-field Optical Nanoscopy* (Tinnefeld, P., Eggeling, C., Hell, S. W., eds) pp. 27–64, Springer, Berlin
52. He, J., Johnson, J. L., Monfregola, J., Ramadass, M., Pestonjamasp, K., Napolitano, G., Zhang, J., and Catz, S. D. (2016) Munc13–4 interacts with syntaxin 7 and regulates late endosomal maturation, endosomal signaling, and TLR9-initiated cellular responses. *Mol. Biol. Cell* **27,** 572–587
53. Hanneken, A., Lin, F. F., Johnson, J., and Maher, P. (2006) Flavonoids protect human retinal pigment epithelial cells from oxidative-stress-induced death. *Invest. Ophthalmol. Vis. Sci.* **47,** 3164–3177